Alma Mater Studiorum · Università di Bologna

Scuola di Scienze
Corso di Laurea in Fisica

Propagation of a Gaussian electromagnetic pulse and laser acceleration

Relatore:

Chiar.mo Prof Graziano Servizi

Correlatore:

Chiar.mo Prof Giorgio Turchetti

Presentata da:

Giulio Bondanelli

Sessione II

Anno Accademico 2012/2013

Ad Alessia

Abstract

By solving the wave equation for an electromagnetic radiation an integral expression for the monochromatic pulse of fixed frequancy ω_0 and for the finite pulse was found, by imposing that in the transversal space of momenta (k_x, k_y) the wave is represented by a Gaussian function $\propto \exp[-w_0^2(k_x^2 + k_y^2)/4]$, where w_0 is the transversal waist.

In order to derive simple analytical expressions for the monochromatic and finite pulses we have performed respectively the paraxial approximation and the factorization approximation.

We have derived, both analytically and numerically, the conditions under which these approximations are to be considered valid. With the aim of color plots we have compared the exact solutions with the approximate solutions.

In the final chapter it is analyzed the motion of a charged particle which interacts with a one-dimensional wave packet, highlighing the main difference when the particle moves in vacuum or in a plasma. In fact, in agreement with Lawson-Woodward theorem, the particle in vacuum cannot gain energy by the direct interaction with the field, while the particle in a plasma, after the passage of the pulse, can be found to have gained momentum.

Sommario

É stata risolta l'equazione d'onda per la radiazione elettromagnetica ed é stata trovata l'espressione (in forma di integrale) per un impulso monocromatico di frequenza angolare ω_0 e per un impulso di durata finita, imponendo che nello spazione dei vettori d'onda (k_x, k_y) l'impulso sia rappresentato da una funzione Gaussiana nella forma $\exp[-w_0^2(k_x^2 + k_y^2)/4]$, dove w_0 rappresenta il waist trasverso.

Per avere un'espressione analitica dell'impulso monocromatico e dell'impulso di durata finita si sono rese necessarie rispettivamente l'approssimazione parassiale e un'approssimazione di fattorizzazione.

Sono state analizzate, sia analiticamente sia numericamente, i limiti entro i quali queste approssimazioni possono essere considerate accurate. Le soluzioni esatte e le soluzioni approssimate sono state confrontate graficamente.

Nel capitolo finale é stato analizzato il moto di una particella carica che interagisce con un pacchetto d'onda unidimensionale, mettendo in luce la fondamentale differenza tra il moto di questa particella nel vuoto e il moto della stessa in un plasma carico. Infatti, in accordo con il teorema di Lawson-Woodward, nel vuoto la particella non puó essere accelerata per interazione diretta con il pacchetto d'onda, mentre nel plasma, a seguito del passaggio del pacchetto, la particella puó aver acquistato energia.

Contents

Introduction

Today one of the main topics both in theoretical and applied research is laser physics. The interest is mainly due to the wide range of applications and experiments that can be carried out and to the limited dimensions of the necessary experimental apparatus. The main and most striking application (which in turn has other applications) is the so-called *laser-driven acceleration* of particles or, more commonly, the *laser-plasma acceleration*. In fact many experiments have shown that it is possible to obtain electron or ion jets by the interaction of ultra-short laser pulses with solid or gaseous targets.

The interest for the particle acceleration by means of the interaction of a laser pulse with matter has grown since the 50s , when the very first proposal of a laser-ion acceleration came from Veksler (1956). The idea was then tested making use of an electric field induced by an electron beam injected into a plasma. In the following years some analytical models were proposed, which involved the isothermal expansion of the plasma in vacuum and the calculation of the field produced by charge separation in order to evaluate if these models were compatible with ion acceleration. In these first attempts the energy of protons or ions was far below 1 MeV. In order to see more significant energies people had to wait until ultra-short pulse and ultra-high-intensity laser would be built. The interest in laser plasma interaction continued to grow until the 70s , when the research in this field was guided by laser-induced nuclear fusion. The first 10 μm CO_2 laser and glass laser were constructed. First laser sources had pulse duration of tens of microseconds and peak power in the kilowatt range. Then with the enhancement of the techniques it was possible to reach picoseconds (10^{-12} s) pulse durations and megawatt peak powers. In the 90s titanium:sapphire laser medium was discovered and the Chirped Pulse Amplification technique (CPA) invented, with which it became possible to exploit materials (Ti:Sa) that store great amount of energy as signal amplificators. With the aid of this new technique ultra-short (<1 ps to few tens of femtoseconds) pulse duration lasers were realized, with peak powers of in the TWs.

With CPA laser it was also possible to drastically reduce the size of lasers, without to compromise on powers. Nowadays, although focused in a ultra-short pulse, state-of-the-art lasers reach petawatt (10^{15} W) level, while multiPW and exawatt (10^{18} W) lasers are in the planning stage.

The attention paid to the laser-plasma acceleration can be understood if we think to the features of this approach in contrast to the traditional particle accelerators. In traditional particle accelerators the acceleration is achieved by electric longitudinal fields induced by radio frequency cavities. However the process of acceleration is limited by the material breakdown threshold ($E_{break} \sim$

50 MV/m), upon which the conduction band elecrons get field-ionized, leading to the damange of the accelerators. In order to get the particles gain higher energies, the number of accelerating elements must be increased. This explains the sometimes remarkable dimensions of traditional accelerators.

Unlike traditional accelerators, laser-plasma acceleration has not the breakdown constraint. In fact, this kind of acceleration makes no use of dielectric materials that can be dameged by ionization. It is given by the interaction with an electromagnetic wave and a plasma which, by definition, is already field-ionized. Tipical values of the fields that intervene in laser-plasma acceleration are of the order of magnitude of TV/m (10^{12} V/m), which is bigger than the typical values of the electric field inside an atom ($\approx 9,2 \cdot 10^{10} A^{1/3}\, V$/m, where A is the mass number).

Before the year 2000 accelerated ion beams of several MeV have been observed in a lot of high-intensity laser-matter interaction experiments making use of different targets, either thick solid targets or gas jets. But they displayed a rather isotropic emission and an extreme angular dispersion, with the resulting low radiance. These reasons made those experiments not attractive for ion acceleration applications. In the year 2000 three important experiments (Clark *et al.*, Maksimchuk *et al.* and Snavely *et al.*) were carried out, with an ultra-intense laser beam impinging on tens of microns thickness targets, either solid or plastic. Protons were detected at the rear side of the targets and they were emitted in a rather well collimated beam with respect to the propagation direction of the laser pulse. At present laser-plasma accelerators are able to produce electron beams of 1 Gev energy over a distance lower than 1 cm and ion beams of several tens of Mev over a distance of some tens of microns. For instance the typical acceleration field for a laser-plasma acceleration is of the order of MV/μm compared to the $\sim$ 10 MV/m of the conventional radio frequency (RF) wave based accelerators.

The idea which lies at the base of laser plasma acceleration is the creation of plasma waves able to give rise to high electric field ($\sim$ TV/m). The particles with the larger charge to mass ratio, i.e. the electrons, are first accelerated. Two main contribution to electron aceleration are given by the ponderomotive force and by *nonlinear Thomson scattering*.

The ponderomotive force takes place when a charged particle is subject to a oscillating inhomogeneous electromagnetic field. When the field is homogeneous in space, after one cycle of oscillation the particle is found in the same point where was at the start of the oscillation. But when the field is inhomogeneous in space the particle experiences a net force which is proportional to the gradient of the square amplitude of the electric field (or vector potential as well). The expression of the ponderomotive force can be derived in many ways. By averaging the Lorentz equation of motion we find that the non-relativistic ponderomotive force is given by $F_p = -(e^2/4m\omega^2)\nabla|E_0|^2$, while the corresponding ponderomotive potential is $U_p = e^2|E_0|^2/4m\omega^2$, where E_0 is the envelope of the electric field.

For the relativistic description of laser-plasma interaction it is usually introduced the *normalized vector potential* $a_0 = eA/m\omega$. From simple calculations it is found that the relativistic gamma factor is given by $\gamma \simeq \sqrt{1 + a_0^2}$. Integrating the equations of motion for a charged particle interacting with a plane wave of angular frequency ω, we find that in the relativistic regime the particle possesses not only a quiver velocity of frequency ω of the first order in a_0 but

also a velocity along the propagation of the laser pulse of the second order in a_0. This velocity is composed of a linear contribution in t and an oscillating contribution with frequency 2ω. This is referred to as the nonlinear Thomson scattering. More precisely when a low-intensity electromagnetic wave of frequency ω is irradiated on an electron, this undertakes an oscillatory motion and it emits characteristic electromagnetic waves of the same frequency ω in turn. When the intensity of the beam increases, a relativistic description of phenomenon is necessary. In this case the nonlinear Thomson scattering takes place and the electron emits electromagnetic waves in the form of higher harmonics. In the relativistic description the expression of the ponderomotive force is the same but for a transformation $m \mapsto \gamma m$.

While electrons are 'directly' accelerated by the laser-matter interaction, the ion acceleration makes use of the electron acceleration. In fact, because of their smaller charge to mass ration, the heaviest protons and ions interact weakly with the laser pulse fields. Ion acceleration is obtained using $\sim$ 1-10μm thickness solid targets. When the laser pulse reach the front side of the target, a cloud of hot electrons is created and it reaches the back side. There have been a lot of disputes about which ions are actually accelerated, if from the front side or from the rear side of the targets. Computer simulations have shown that when electrons reach the rear side of the target they give rise to strong electric fields by charge separation and these field get the ion from the rear side of the target ionized, leaving the target. The accelerated protons that are observed in real experiments together with ions come from the thin layer of water vapour which lie on the target (*contaminants*). The main mechanisms of electron and ion acceleration are described in more detail in Chapter 2.

The small dimensions of laser based accelerators compared to that of conventional accelerators make the laser-plasma acceleration techniques attractive for a lot of applications. All over the world protons accelerators have been built for cancer therapy. The peculiar features of proton beams is to let the tissues near the cancer not irradiated. For mediacal therapy protons with energies up to 250 MeV are required and now new geometries of the targets are studied in order to get more collimated and monochromatic beams. Other important applications are the *Fast Ignition*, X-rays production and proton *imaging*.

Chapter 1

Plasma parameters and laser acceleration regimes

1.1 Plasma parameters

Debye length A fundamental parameter for the description of a plasma is the Debye length. The description of a plasma, in fact, is not exhausted by remarking its elevate ionization, but also it makes use of the concept of *quasineutrality*.

All charges in a plasma can interact with the others through the long range electric potential $V \sim 1/r$. However charges are freely moving, so that in the neighborhood of a positive charge there is a rarefaction of positive charges and an accumulation of negative ones. As a consequence, after a certain distance r_s from the positive charge, this latter is shielded by the negative ones and the electric potential is nearly zero. If we label with r_s the distance at which the shielding action becomes relevant it can be easily understood that volumes with linear dimensions greater than r_s have a charge nearly null inside them. So, if $Q(r)$ is the total charge inside the sphere of radius r, the condition of *quasineutrality* is given by $Q(r_s) \approx 0$.

We want now determine the order of magnitude of r_s. Suppose we have an hydrogen plasma (so composed only by protons and electrons) with uniform density n_0 of positive and negative charges. Suppose moreover that a positive charge $e_0 > 0$ is inserted in the point of coordinate $\mathbf{r} = 0$. In general, the charge density n_i and n_e of protons and electrons respectively after having inserted the charge e_0 will not be equal to the initial one n_0. The main hypothesis that is done in this case is that the new distribution of charges is in thermal equilibrium at a given temperature T, and so charge densities follow Boltzmann distribution. By Maxwell's equation we have (in Gaussian units)

$$\nabla \cdot \mathbf{E} = -\nabla\Phi = 4\pi e(n_i - n_e) + 4\pi e_0 \delta(\mathbf{r}), \tag{1.1}$$

where e is the magnitude of the electron charge and n_i and n_e are given by the Boltzmann distribution law (with $\beta = 1/kT$)

$$n_i = n_0 \exp(-\beta e\Phi), \tag{1.2a}$$
$$n_e = n_0 \exp(\beta e\Phi). \tag{1.2b}$$

Inserting 1.2a and 1.2b in 1.1 we obtain the equation for the potential Φ

$$\begin{aligned}\nabla^2\Phi &= 4\pi n_0 e[\exp(\beta e\Phi) - \exp(-\beta e\Phi)] - 4\pi e_0\delta(\mathbf{r}) \\ &= 8\pi n_0 e \sinh(\beta e\Phi) - 4\pi e_0\delta(\mathbf{r}).\end{aligned} \tag{1.3}$$

If we now make the assumption, whose validity will be checked later, that $\beta e\Phi \ll 1$ the approximated equation for Φ is

$$\nabla^2\Phi = 8\pi\beta e^2 n_0\Phi - 4\pi e_0\delta(\mathbf{r}) + O((\beta e\Phi)^3). \tag{1.4}$$

Using the radial component of the laplacian in spherical coordinates and making the substitution $\lambda = (8\pi\beta e^2 n_0)^{-1/2}$ (and neglecting third order terms) we can write the 1.4 as follows

$$\frac{d^2}{dr^2}(r\Phi) = \frac{r\Phi}{\lambda^2} - 4\pi e_0 r\delta(\mathbf{r}). \tag{1.5}$$

Since, by the therory of generalized function, the second term on the right hand side is identically zero, the solution of 1.5 reads as

$$\Phi(r) = e_0\frac{\exp(-r/\lambda)}{r} = e_0\frac{\exp(-\sqrt{2}r/\lambda_D)}{r}, \tag{1.6}$$

where we defined the *Debye length* as

$$\lambda_D = \sqrt{2}\lambda = (4\pi\beta e^2 n_0)^{-1/2}. \tag{1.7}$$

A numerical evaluation gives $\lambda_D[\mu m] = 1,59\cdot 10^{-14}\sqrt{T[K]/n_0[cm^{-3}]}$.
In vacuum ($n_0 = 0$, $\lambda_D \to \infty$) we find the ordinary Coulomb potential.

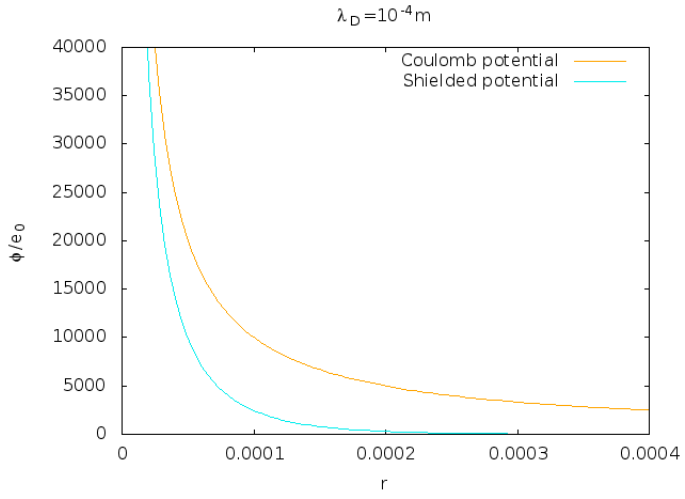

Figure 1.1: Comparison between the trends of shielded potential and Coulomb potential for $\lambda_D = 1\mu$m. r is measured in cm while ϕ/e_0 is measured in cm^{-1}.

We can now calculate, with the aim of Gauss theorem, the total charge inside a sphere S of radius r and see that for a large radius r this charge tends to zero,

according to the property of *quasineutrality*, typical of plasmas. If we assume a spherical symmetry for the radial component of the electric fiels $\mathbf{E}$ we have

$$q(r) = \int_{S(r)} \mathrm{d}\, V \rho(r') = \frac{1}{4\pi} \int_{S(r)} \mathrm{d}\, V (\nabla \cdot \mathbf{E}) = \frac{1}{4\pi} \int_{S(r)} \mathbf{E} \cdot \frac{\mathbf{r}}{r} \mathrm{d}\, \sigma = r^2 E_r(r).$$

The radial component of the electric field is given by (in terms of λ)

$$E_r(r) = -\frac{\partial V}{\partial r} = e_0 \exp(-r/\lambda) \left[\frac{1}{\lambda r} + \frac{1}{r^2} \right],$$

and so

$$q(r) = e_0 \exp(-\sqrt{2} r/\lambda_D) \left[\frac{\sqrt{2} r}{\lambda} + 1 \right] \tag{1.8}$$

Two indicative limits can be written:

$$\lim_{\lambda_D \to \infty} q(r) = e_0 \tag{1.9a}$$
$$\lim_{\lambda_D \to 0} q(r) = 0. \tag{1.9b}$$

The limit 1.9a accounts for the point-like charge put in the origin, while 1.9b accounts for the fact that putting a charge e_0 in the origin causes a redistribution of a charge $-e_0$ in the whole space around it. From these results we can write the charge $q(r)$ as the sum of a point-like charge e_0 and a regular charge $q_{reg}(r)$

$$q(r) = e_0 + q_{reg}(r)$$

and the same can be done with the electric field $E_r(r)$ and the charge density $\rho(r)$

$$E_r(r) = r^{-2} e_0 + E_{r,reg}(r) \tag{1.10}$$
$$\rho(r) = e_0 \delta(r) + \rho_{reg}(r), \tag{1.11}$$

where

$$\rho_{reg}(r) = \frac{e_0}{2\pi\lambda_D^2} \frac{\exp(-\sqrt{2} r/\lambda_D)}{r}.$$

The contribution of the regular term of the charge density goes to zero when $\lambda_D \to \infty$. In fact, in this case, only the singular term of the charge density gives its contributon.

In this derivation we made use of statistical mechanics, that is, of the Boltzmann distribution law to describe the charge density of particles in regions of linear dimensions of the order of the Debye length. This approach makes sense if $d \ll \lambda_D$, where d is the mean distance of the particles. For $d \sim n^{-\frac{1}{3}}$ we can write the formal expression of the condition of *quasineutrality*

$$n\lambda_D^3 \gg 1. \tag{1.12}$$

Evaluating the term $e\beta\Phi$ for $r = d$ we obtain

$$(e\beta\Phi)_{r=d} = e^2\beta\frac{\exp(-\sqrt{2}d/\lambda_D)}{d} \simeq \frac{e^2\beta}{d} \simeq e^2\beta n^{1/3} \simeq \left(\frac{d}{\lambda}\right)^2 \ll 1,$$

finding that the assumption we made in order to obtain 1.4 is completely justified.

Plasma waves Another fundamental aspect of plasma is its behaviour in interactiong with electromagnetic radiation. In fact, an electromagnetic wave which propagates in a plasma generate density waves. This can be seen using the continuity equation, Newton's second law and Poisson equation

$$\frac{\partial n}{\partial t} + \nabla \cdot (n\mathbf{v}) = 0 \tag{1.13a}$$

$$\rho\frac{d\mathbf{v}}{dt} = ne\mathbf{E} \tag{1.13b}$$

$$\nabla \cdot \mathbf{E} = 4\pi ne, \tag{1.13c}$$

where

$$\frac{d}{dt} = \frac{\partial}{\partial t} + \sum_k v_k \frac{\partial}{\partial x_k},$$

$n(\mathbf{x}, t)$ is the number of particles per unit volume, $\rho(\mathbf{x}, t)$ is the mass per unit volume, $\mathbf{v}(\mathbf{x}, t)$ is the velocity of a infinitesimal volume around $\mathbf{x}$ at time t and e is the signes value of the particles involved. We find easily that the equilibrium state is given by $n = n_0 = const$, $\mathbf{v} = 0$ and $\mathbf{E} = 0$.

If we now perturb the equilibrium density $n = n_0 + n_1$ we find a perturbation in the electric field $\mathbf{E} \equiv \mathbf{E}_\epsilon$ and a perturbation in the velocity of charges $\mathbf{v} \equiv \mathbf{v}_\epsilon$. As long as $\rho = mn$, with m the mass of a single particle, we find that the linearized 1.14 are given by

$$\frac{\partial n_1}{\partial t} + n_0\nabla \cdot \mathbf{v} = 0 \tag{1.14a}$$

$$m\frac{\partial \mathbf{v}}{\partial t} = e\mathbf{E} \tag{1.14b}$$

$$\nabla \cdot \mathbf{E} = 4\pi n_1 e, \tag{1.14c}$$

Deriving 1.14a with respect to t and using 1.14b we obtain

$$\frac{\partial^2 n_1}{\partial t^2} = -n_0\frac{\partial}{\partial t}(\nabla \cdot \mathbf{v}) = -\frac{n_0 e}{m}\nabla \cdot \mathbf{E}. \tag{1.15}$$

Using the Poisson equation 1.14c , the equation 1.15 is reduced to the typical harmonic motion equation for the perturbation density $n_\epsilon = n - n_0$

$$\frac{\partial^2 n_1}{\partial t^2} + \omega_p^2 n_1 = 0, \tag{1.16}$$

where it has been defined the plasma frequency as

$$\omega_p^2 = \frac{4\pi e^2 n_0}{m}.$$

In a similar way it can be shown that also the velocity obeys the same equation

$$\frac{\partial^2 \mathbf{v}}{\partial t^2} + \omega_p^2 \mathbf{v} = 0.$$

Refractive index In linear approximation the refractive index of the plasma can be calculated. The equations for the magnetic induction $\mathbf{B}$, for the momentum and for the current density $\mathbf{j}$ for small perturbations must hold:

$$\nabla \times \mathbf{B} = \frac{4\pi}{c}\mathbf{j} + \frac{1}{c}\frac{\partial \mathbf{E}}{\partial t} \tag{1.17a}$$

$$m\frac{\partial \mathbf{v}}{\partial t} = e\mathbf{E} \tag{1.17b}$$

$$\mathbf{j} = n_0 e \mathbf{v} \tag{1.17c}$$

$$\nabla \times \mathbf{E} = -\frac{1}{c}\frac{\partial \mathbf{B}}{\partial t}. \tag{1.17d}$$

Searching for the solutions of equations 1.17 in the form

$$\mathbf{E}(\mathbf{x}, t) = \mathbf{E}_0 \exp(-i\omega t) \equiv \mathbf{E}_0^* \exp[i(\mathbf{k}\cdot\mathbf{x} - \omega t)] \tag{1.18}$$

and using equations 1.17a , 1.17b , 1.17c we find that

$$\nabla \times \mathbf{B} = \frac{4\pi}{c}\frac{n_0 e^2}{m}\frac{i}{\omega}\mathbf{E} - \frac{i\omega}{c}\mathbf{E} = -\frac{i\omega}{c}\left(1 - \frac{\omega_p^2}{\omega^2}\right)\mathbf{E}. \tag{1.19}$$

Deriving 1.19 with respect to time and using the equation for the curl of the electric field 1.17d we obtain

$$\nabla \times \nabla \times \mathbf{E} = \frac{\omega^2}{c^2}\left(1 - \frac{\omega_p^2}{\omega^2}\right)\mathbf{E}.$$

Since for fields in the form 1.18 the relation $\nabla \times \mathbf{E} = i\mathbf{k} \times \mathbf{E}$ holds, we have

$$\mathbf{k} \times \mathbf{k} \times \mathbf{E} = -\frac{\omega}{c^2}\left(1 - \frac{\omega_p^2}{\omega^2}\right)\mathbf{E} \tag{1.20}$$

If we take propagation direction of the electromagnetic wave in the plasma along the z axis ($\mathbf{k} = k\hat{\mathbf{z}}$), equation 1.20 can be put in the form

$$\begin{pmatrix} \omega^2 - \omega_p^2 - k^2c^2 & 0 & 0 \\ 0 & \omega^2 - \omega_p^2 - k^2c^2 & 0 \\ 0 & 0 & \omega^2 - \omega_p^2 \end{pmatrix} \begin{pmatrix} E_x \\ E_y \\ E_z \end{pmatrix} = \begin{pmatrix} 0 \\ 0 \\ 0 \end{pmatrix} \tag{1.21}$$

A solution of the vectorial equation 1.21 is $E_x = E_y = 0$ and $\omega^2 = \omega_p^2$, which corresponds to a situation in which the electric field oscillates in the z direction. For the indetermination of k the phase velocity $v_\phi = \omega/k$ can take any value, while the group velocity $v_g = \frac{\partial \omega}{\partial k} = 0$. This means that this kind of waves do not propagates. They are nothing but plasma oscillation and, since $\mathbf{E}$ is parallel to $\mathbf{k}$, they are not associated with magnetic perturbation but only to electrostatic ones.

The secondo solution of 1.21 describes transversal waves and is $E_z = 0$ and

$$\omega^2 = \omega_p^2 + k^2 c^2, \tag{1.22}$$

where this latter equation gives the dispersion relation. These kind of wave have a group velocity given by

$$v_g = c\left(1 - \frac{\omega_p^2}{\omega^2}\right)^{1/2} \tag{1.23}$$

and a phase velocity given by

$$v_\phi = \frac{c}{n_{\text{refr}}} = c\left(1 - \frac{\omega_p^2}{\omega^2}\right)^{-1/2}. \tag{1.24}$$

Hence, in this case, the plasma medium is characterized by a refractive index equal to

$$n_{\text{refr}} = \frac{c}{v_\phi} = \left(1 - \frac{\omega_p^2}{\omega^2}\right)^{1/2}. \tag{1.25}$$

Skin depth and critical density We note that the refractive index n_{refr} can be either real or complex, depending on the frequency ω of the propagating wave. From 1.22 we see that the magnitude of the wave number k is given by

$$k = \left(\frac{\omega^2 - \omega_p^2}{c^2}\right)^{1/2}. \tag{1.26}$$

Thus, we see that if $\omega > \omega_p$ both the refractive index and the wave number are real. Therefore, in this case, we deal with a wave which effectively propagates within the plasma with frequency ω and wave number k.

If $\omega < \omega_p$, then the refractive index and the wave number are pure imaginary numbers.

If we now substitute the complex wave number

$$k = i\left(\frac{\omega_p^2 - \omega^2}{c^2}\right)^{1/2}$$

in the expression for the monochromatic plane wave 1.18 we see that it represents an evanescent wave, which propagates with frequency ω but damped in space

$$\mathbf{E} = \mathbf{E}_0^* e^{i\omega t} \exp\left[-\left(\frac{\omega_p^2 - \omega^2}{c^2} \right)^{1/2} z \right] = \mathbf{E}_0^* e^{-i\omega t} e^{-z/l_s},$$

where the *skin depth* has been defined and it represents the length at which the field amplitude has been damped by a factor $1/e$

$$l_s = \left(\frac{c^2}{\omega_p^2 - \omega^2} \right)^{1/2} = \frac{c}{\omega} \left(\frac{\omega_p^2}{\omega^2} - 1 \right)^{-1/2} = \frac{\lambda}{2\pi} \left(\frac{\omega_p^2}{\omega^2} - 1 \right)^{-1/2}. \tag{1.27}$$

If we now call *critical density* the density at which $\omega_p = \omega$

$$n_c = \frac{m\omega}{4\pi e^2} \tag{1.28}$$

for $n < n_c$ we have $\omega > \omega_p$ and the plasma is transparent and lets waves propagate within it; conversely, if $n > n_c$ then $\omega < \omega_p$ and the plasma medium becomes opaque to radiation. Expressing 1.27 in function of the particle density n of the plasma we get

$$l_s = \frac{\lambda}{2\pi} \left(\frac{n}{n_c} - 1 \right)^{-1/2}. \tag{1.29}$$

For low frequencies $\omega \ll \omega_p$ (that is, $n \gg n_c$) the approximate relation reads

$$l_s \simeq \frac{\lambda}{2\pi} \left(\frac{n_c}{n} \right)^{1/2} = \frac{\lambda\omega}{2\pi\omega_p} = \frac{c}{\omega_p}. \tag{1.30}$$

1.2 Acceleration regimes

There are different regimes of laser based particle acceleration, depending on the kind of particle accelerated (electrons or ions) and on the range of intensity at which the acceleration takes place. In the following the main regimes of electrons and ion acceleration are described in more detail.

Laser Weak-Field Acceleration (LWFA) Electron acceleration generally takes place in an underdense plasma ($n_e < n_c$) like gas jets. In LWFA the electron acceleration is brought about by the ponderomotive force. When the rising edge of the pulse reach the target the electrons of the plasma experience a force proportional (with the minus sign) to the gradient of the intensity. After the pulse have overtaken the particle, this meet the falling edge and experiences an opposite force. In this way, if the parameters of the plasma are well-combined, a wave propagates all along the plasma and electrons can be accelerated to 1 Gev in a few millimeters.

Self-focusing When the relativistic description of the motion of the electrons of the plasma becomes important we have the self-focusing, an peculiar effect which increase the interaction length between the pulse and the plasma. The refractive index is given by $n_{\text{refr}}^2 = 1 - \omega_p^2/\omega^2$ (where the relativistic description imposes $\omega_p^2 \mapsto \omega_p^2/\gamma$). Both the increasing drift velocity of the electrons and the ponderomotive force that pushes away electrons from the focus axis making the plasma density to decrease make the refractive index increase. In that way plasma acts as a convergent lens and let the pulse propagates along distances greater that z_R, contrasting the defocusing. The power necessary to observe the phenomenon are easily available at present.

Target Normal Sheath Acceleration (TNSA) In this regime, an electromagnetic wave interacts with an overdense plasma $n > n_c$ constituted by a solid foil of a few micrometers thickness $l > l_s$. Long before the peak of the laser pulse has reached the target an energetic and high-temperature electron contribution is created which propagated into the foil and reaches the rear side of the target. If the target is thin enough (typically a few μm for a metal foil) the electrons reach the back surface without considerable energy loss.

The main part of the hot electrons are trapped near the back of the target because of the electric field generated by this charge separation and form a sheath right at the rear side of the foil. The electron distribution can shield the positive charge at least after a distance of a Debye length λ_D and the available electric field due to this uncompensated charge is of the order of 10^{12} V/m. Such fields can ionize the atoms present at the back surface of the target. As long as they are created by ionization they are accelerated perpendicular to the conducting surface of the target.

In order to improve the monochromaticity of the ion beams an additional layer of *contaminants* (hydrocarbons or water vapour) deposited at the back surface of the target can be used. In this way, the strong fields created accelerate either the heavy metal ions and the lighter protons which comes from the contaminants (containing hydrogen). In this case, while the heavy metal ions are accelerated in every directions, the hydrogen ions (protons) are accelerated mainly forward in the direction normal to the target surface. In order to achieve a 10^{10} proton bunch it is sufficient to have a $0,02\,\mu$m thick contaminant layer. This enables the protons in this layer to have nearly the same initial condition, so ensuring a better energy dispersion than in the case of a single monomaterial foil.

Radiation Pressure Acceleration (RPA) While in the TNSA the heating of the electrons was the main mechanism to accelerate ions, in RPA regime the ponderomotive force is the cause of the ion acceleration. PIC simulations shows that for pulse intensities $I \geq 5 \cdot 10^{21}\,\text{W/cm}^2$ an acceleration regime different from TNSA starts to dominate and RPA is now one of the possible means to accelerate ions up to relativistic energies (Gev/nucleon). In order to achieve Gev/nucleon energies high-intensity lasers ($I \geq 10^{23}\,\text{W/cm}^2$) are needed. Such lasers are not available yet, but it has been demonstrated that RPA regime can dominate over TNSA at lower intensities if it is used circularly polarized light instead of linearly polarized one.

If thick targets are used the ponderomotive force is effective only on a thin

layer of the target and the acceleration of ions is due to the strong electric field E_x (in the direction of propagation of the pulse) arisen from the electron displacement generated by the ponderomotive force. This configuration is referred to as "Hole Boring". After the ions have overcome the region of accelerations they are not able to gain energy any more.

If thin targets are used the laser is able to repeat the acceleration stage. After the first acceleration, ions do not pile up to a singular density because it is as if they constitute the whole target. The laser repeated acceleration stages act on the electrons but, since the motion of ions is strictly bound to that of the electron, the target can be considered as a rigid object. In fact the "flying mirror" model of RPA consider the motion of particles as a rigid body pushed by the radiation pressure $P = 2I/c$ of the laser electromagnetic wave.

Magnetic Vortex Acceleration (MVA) The MVA regime requires targets at critical or slightly overcritical density ($n \simeq n_c$). On the experimental side, hydrogen gas jets are approaching the required parameters, and hydrogen rich aerogels might also be suitable. In this density range the medium is relativistically transparent, the laser pulse drills a channel where the electrons acceleration is mainly due to the ponderomotive force. At the exit of the target, the proton acceleration is due to an inductive electric force, caused by the expansion of a magnetic vortex created during the electron acceleration stage, and to the electron cloud moving forward as in TNSA.

Chapter 2

Gaussian pulse

The Gaussian pulse is particular kind of electromagnetic field which is obtained by imposing as initial condition in the focus ($t = 0$, $z = 0$) an expression in the form $E(x, y, 0, 0) \propto \exp[-(x^2 + y^2)/w_0]$. The time evolution of the field is given by a suitable integral expression which satisfies exactly to the wave equation. Both the monochromatic case and the finite pulse case are analyzed. We cannot get analytical expression of these fields unless we use inifinite series. Analytical expressions can be deduced by making the paraxial approximation, discussed below.

2.1 Solutions of the wave equation

We recall now the Maxwell's equation with sources (in Gaussian units):

$$\nabla \cdot \mathbf{E} = 4\pi\rho \tag{2.1a}$$

$$\nabla \times \mathbf{E} = -\frac{1}{c}\frac{\partial \mathbf{B}}{\partial t} \tag{2.1b}$$

$$\nabla \cdot \mathbf{B} = 0 \tag{2.1c}$$

$$\nabla \times \mathbf{B} = \frac{4\pi}{c}\mathbf{j} + \frac{1}{c}\frac{\partial \mathbf{E}}{\partial t} \tag{2.1d}$$

The equations for the potentials reads:

$$\mathbf{B} = \nabla \times \mathbf{A} \tag{2.2a}$$

$$\mathbf{E} = -\nabla\phi - \frac{1}{c}\frac{\partial \mathbf{A}}{\partial t} \tag{2.2b}$$

There is a certain freedom in the choice of the potentials, since the fields don't change after trasformations

$$\mathbf{A} \longrightarrow \mathbf{A} + \nabla S \tag{2.3a}$$

$$\phi \longrightarrow \phi - \frac{\partial S}{\partial t} \tag{2.3b}$$

where $S = S(\mathbf{r}, t)$ is a scalar function. If we choose the gauge so that

$$\nabla \cdot \mathbf{A} = -\frac{1}{c}\frac{\partial \phi}{\partial t}$$

we can write the wave equations for the potentials as:

$$\left(\nabla^2 - \frac{1}{c^2}\frac{\partial^2}{\partial t^2}\right)\mathbf{A} = -\frac{4\pi}{c}\mathbf{j} \tag{2.4a}$$

$$\left(\nabla^2 - \frac{1}{c^2}\frac{\partial^2}{\partial t^2}\right)\phi = -4\pi\rho. \tag{2.4b}$$

In vacuum we can set $\phi = 0$ so that the gauge becomes $\nabla \cdot \mathbf{A} = 0$. The electric and magnetic fields are given respectively by:

$$\mathbf{B} = \nabla \times \mathbf{A} \tag{2.5a}$$

$$\mathbf{E} = -\frac{1}{c}\frac{\partial \mathbf{A}}{\partial t} \tag{2.5b}$$

and, since $\mathbf{j} = 0$ and $\rho = 0$, the potential vector satisfies the wave equation

$$\left(\nabla^2 - \frac{1}{c^2}\frac{\partial^2}{\partial t^2}\right)\mathbf{A} = 0. \tag{2.6}$$

It is well known that both the electric and the magnetic fields satisfy the same wave equation 2.6. This can be derived from Maxwell's equations 2.1a - 2.1d or by deriving with respect to space or time 2.6 in order to recover the fields 2.5a and 2.5b, given that the fields are sufficiently regular (at least C^2). Thus either $\mathbf{E}$, $\mathbf{B}$ and $\mathbf{A}$ satisfy the same wave equation 2.6.

Now it is useful to introduce another notation $E = E(x, y, z, t)$ to indicate whichever component of the electric, the magnetic or the potential vector field. We want to deduce an expression of E with the proper initial condition which fits the wave equation, that now can be written as:

$$\left(\nabla^2 - \frac{1}{c^2}\frac{\partial^2}{\partial t^2}\right)E(x, y, z, t) = 0 \tag{2.7}$$

The following discussion can be applied to $\mathbf{E}$, $\mathbf{B}$ and $\mathbf{A}$. However at the end of some calculations we will identify E with some component of the electric field and extract the expression for all components of the electromagnetic fields by means of Maxwell's equations. There are two kind of suitable expressions for E which satisfy the wave equation. We present the main features of each one.

First solution The first integral expression for the field E we can deduce which exactly satisfy the equation 2.7 is the following:

$$E(x,y,z,t) = \frac{1}{(2\pi)^3}\int_{-\infty}^{+\infty} dk_x\, dk_y\, dk_z\, \hat{E}(k_x,k_y,k_z)e^{i(k_x x+k_y y+k_z z-\omega t)} \tag{2.8}$$

with the angular frequency given by

$$\omega = \sqrt{k_x^2+k_y^2+k_z^2}. \tag{2.9}$$

We have defined the Fourier transform of a function $f(\mathbf{z})$ the function $\hat{f}(\mathbf{k}) = \int_{-\infty}^{+\infty} f(\mathbf{z})\exp(-i\mathbf{z}\cdot\mathbf{k})\, d\mathbf{z}$ and consequently the inverse Fourier transform of $\hat{f}(\mathbf{k})$ the function $f(\mathbf{z}) = (2\pi)^{-D}\int_{-\infty}^{+\infty}\hat{f}(\mathbf{k})\exp(i\mathbf{z}\cdot\mathbf{k})\, d\mathbf{k}$ (the normalization constant before the integrals can be chosen as you like but their product must give the result $(2\pi)^{-D}$ where D is half the dimension of the phase space). If in the solution 2.8 we set $t = 0$ we easily see that $\hat{E}(k_x,k_y,k_z)$ is nothing but the Fourier transform of the initial condition $E(x,y,z,0)$:

$$\hat{E}(k_x,k_y,k_z) = \int_{-\infty}^{+\infty} \mathrm{d}x\,\mathrm{d}y\,\mathrm{d}z\, E(x,y,z,0)\, e^{-i(k_x x+k_y y+k_z z)} \tag{2.10}$$

Second solution The second integral expression which satisfies 2.7 reads:

$$E(x,y,z,t) = \frac{1}{(2\pi)^3}\int_{-\infty}^{+\infty} \mathrm{d}k_x\,\mathrm{d}k_y\,\mathrm{d}k_z\, \hat{E}(k_x,k_y,k_z)e^{i(k_x x+k_y y+z\sqrt{k_z^2-k_x^2-k_y^2}-\omega t)}. \tag{2.11}$$

We can note that in this case the field is monochromatic. In fact the angular frequency is now given by:

$$\omega = ck_z. \tag{2.12}$$

If we set $z = 0$ we see that $\hat{E}(k_x,k_y,k_z)$ is the Fourier transform of the field $E(x,y,0,t)$:

$$\hat{E}(k_x,k_y,k_z) = c\int_{-\infty}^{+\infty} \mathrm{d}x\,\mathrm{d}y\,\mathrm{d}z\, E(x,y,0,t)\, e^{-i(k_x x+k_y y-k_z ct)} \tag{2.13}$$

If we use the first solution we can set the field E for $t = 0$, for example in the form of a Gaussian transversal profile $\propto \exp[-(x^2+y^2)/w_0]$, calculate its Fourier transform analytically and then its time evolution in an approximate way. If we use the second solution of the wave equation we need to know $\hat{E}(k_x,k_y,k_z)$ in order to obtain the time evolution of E, but $\hat{E}(k_x,k_y,k_z)$ if a function of the time evolution of E at $z = 0$, so that it is impossible to tackle the problem. To overcome it an expression for $\hat{E}(k_x,k_y,k_z)$ will be assigned. In this way we will be able to obtain an approximate analytical expression for $E(x,y,z,t)$ (and for its initial condition $E(x,y,z,0)$ of course).

2.2 Monochromatic Gaussian pulse

If we want to have an expression which represents a rigorously monochromatic wave of frequency k_0 we have to choose the second solution 2.11, since in this case the frequency is given by $\omega_0 = ck_0$. If we had choosen the first solution, even after having set $k_z = k_0$, we would have found by 2.9 a dispersion in frequency around the central frequency ω_0:

$$\omega = \omega_0 \left(1 + \frac{k_x^2 + k_y^2}{k_0^2}\right)^{1/2}. \tag{2.14}$$

Even if the first solution does not provide an expression for a monochromatic wave we can perform some limits to see how the two solutions are related to each other. As we have highlighted above, unlike for the second solution, if we deal with the first solution we can assign an initial condition $E(x, y, z, 0)$ and calculate the Fourier transform. The typical choice one makes is:

$$E(x, y, z, 0) = \exp\left[-\frac{(x^2 + y^2)}{w_0^2}\right] f(z) e^{ik_0 z}, \tag{2.15}$$

where $f(z)$ is a rapidly decreasing or compactly supported function and represents the longitudinal modulation of the field, while $\exp(ik_0 z)$ is a simple phase. The Fourier tranform of 2.15 reads:

$$\hat{E}(k_x, k_y, k_z) = \pi w_0^2 \exp\left[-\frac{w_0^2}{4}(k_x^2 + k_y^2)\right] \hat{f}(k_z - k_0). \tag{2.16}$$

If we substitute 2.16 in 2.10 we get an implicit expression of the time evolution of the field E according to 2.8, given the initial condition 2.15. In order to understand under which conditions a monochromatic wave can be obtained from the first solution we set for example

$$f(z) = e^{-z^2/w_z^2}, \tag{2.17}$$

so that we get

$$\hat{f}(k_z - k_0) = \sqrt{\pi w_z^2} e^{-w_z^2 k_z^2/4}. \tag{2.18}$$

By definition, a monochromatic wave is represented, in configuration space, by an infinite wave of constant longitudinal amplitude and, in momentum space, by a Dirac delta centered in the wave number $k_0 = \omega_0/c$. It is clear that we recover a monochromatic wave for $f(z) \longrightarrow 1$, i.e. in the limit $w_z \longrightarrow \infty$ (it is only a necessary condition, as we next see). If this limit is performed we can write:

$$\lim_{w_z \to \infty} \hat{f}(k_z - k_0) = 2\pi(k_z - k_0). \tag{2.19}$$

The limit $w_z \longrightarrow \infty$ is not sufficient. Along with it, we have to perform the limit $w_0 \longrightarrow \infty$ in 2.15 and 2.16:

$$\lim_{w_0\to\infty}\left\{\pi w_0^2\exp\left[-\frac{w_0^2}{4}(k_x^2+k_y^2)\right]\right\}=(2\pi)^2\,\delta(k_x)\,\delta(k_y). \tag{2.20}$$

Putting together 2.19 and 2.20 in 2.16 and substituting the resulting expression in 2.8 we get the monochromatic wave:

$$E(x,y,z,t)=\int_{-\infty}^{+\infty}\mathrm{d}k_x\,\mathrm{d}k_y\,\mathrm{d}k_z\,\delta(k_x)\,\delta(k_y)\,\delta(k_z-k_0)\,e^{i(xk_x+yk_y+zk_z-ct\sqrt{k_x^2+k_y^2+k_z^2})}$$

$$=e^{ik_0(z-ct)}. \tag{2.21}$$

Another way of tackling the problem is to observe that in order to have a rogorously monochromatic pulse we should have for example:

$$\hat{E}(k_x,k_y,k_z)=\tilde{E}(k_x,k_y)\,(2\pi)\,\delta\Big(k_x-\sqrt{k_0^2-k_x^2-k_y^2}\Big), \tag{2.22}$$

supplied with the condition that $\tilde{E}(k_x,k_y)=0$ for $k_x^2+k_y^2>k_0^2$. If we put this expression in 2.8 we get:

$$E(x,y,z,t)=\frac{1}{(2\pi)^2}\int_{-\infty}^{+\infty}\mathrm{d}k_x\,\mathrm{d}k_y\,\tilde{E}(k_x,k_y)\,e^{i(xk_x+yk_y+z\sqrt{k_0^2-k_x^2-k_y^2}-k_0\,ct)}, \tag{2.23}$$

which is essentially equivalent to the second solution 2.11 after an integration in k_z with a Dirac delta $\delta(k_z-k_0)$.

We recall that in the second solution the initial condition $E(x,y,z,0)$ cannot be obtained in an analytical way. This statement is supported by the fact that, in the case last examined, if we still make choices similar to 2.17 and 2.18, the necessary limit for a monochromatic pulse is given by:

$$\hat{E}(k_x,k_y,k_z)=\lim_{w_z\to\infty}\tilde{E}(k_x,k_y)\,\sqrt{\pi w_z^2}\,\exp\left[-\frac{w_z^2}{4}\Big(k_z-\sqrt{k_0^2-k_x^2-k_y^2}\Big)^2\right] \tag{2.24}$$

If we want to recover the initial condition $E(x,y,z,0)$ we have to inverse Fourier transform 2.24, but the calculation doen not provide an analitycal result. This last case, though it derives from the first approach, is equivalent to the second solution. Thus we have shown that in the first approach the initial condition $E(x,y,z,0)$ is expressed analytically, while in the second approach we cannot write it in an analytical way.

If we analyze more in detail the dispersion in frequency 2.14 related to the first solution of the wave equation we can estimate it in terms of more fundamental parameters which will be useful in the next sections. If we choose a transversal Guassian profile $\propto\exp[(x^2+y^2)/w_0^2]$ the Fourier transform is

$\propto \exp[-w_0^2(k_x^2+k_y^2)/4]$. In this case the equation $\langle k_x^2+k_y^2\rangle = 4/w_0^2$ holds. From equation 2.14 we get:

$$\frac{\omega^2-\omega_0^2}{\omega_0^2} = \frac{k_x^2+k_y^2}{k_0^2} \sim \frac{4}{k_0^2\, w_0^2} = \frac{\lambda_0^2}{\pi^2 w_0^2} \equiv \epsilon^2. \tag{2.25}$$

We see that if we deal with the first solution of the wave equation, which has in general a dispersion around the central frequency ω_0, the smaller is the parameter ϵ the more monochromatic the wave is. We can reach this limit by fixing the transversal waist w_0 and by letting the central wave length $\lambda_0 = 2\pi/k_0$ go to zero, or by fixing a frequency ω_0 and by letting the transversal waist go to infinity (as we have already stated before).

2.2.1 Paraxial approximation

In this section we obtain an analitycal expression for the monochromatic pulse. If we want a wave with central frequency $\omega_0 = ck_0$ we have to use the second solution 2.11. Nevertheless the first solution reduces to the monochromatic pulse in the limit $\epsilon \longrightarrow 0$, so that in this limit the two approaches coincide. It is ϵ itself which constitutes the crucial parameter which characterizes the goodness of the *paraxial approximation*, that we are next to see.

If we deal with the second formulation it is of no use to assign an initial condition $E(x,y,z,0)$. For that reason we have to set an expression for $\hat{E}(k_x,k_y,k_z)$. Since we want a monochromatic Gaussian pulse the most natural choice is given by 2.16, with $\hat{f}(k_z-k_0)$ given by a Dirac delta $2\pi\delta(k_z-k_0)$ because of the monochromaticity of the pulse. The implicit expression of the time evolution of this pulse is given by 2.11:

$$E(x,y,z,t) = \frac{\pi w_0^2}{(2\pi)^2}\int_{-\infty}^{+\infty} \mathrm{d}k_x\,\mathrm{d}k_y\, \exp\left[-\frac{w_0^2}{4}(k_x^2+k_y^2)\right] \exp\left[i(xk_x+yk_y+z\sqrt{k_0^2-k_x^2-k_y^2}-k_0\,ct)\right] \tag{2.26}$$

It is clear that this integral is solvable only numerically. In order to get a simple analytical expression we have to do the so-called paraxial approximation. We set

$$\epsilon = \frac{2}{k_0 w_0} = \frac{\lambda_0}{2\pi w_0} = \frac{w_0}{z_R} \tag{2.27}$$

and introduce a characteristic length, called *Rayleigh length*, defined by

$$z_R = \frac{k_0 w_0^2}{2}. \tag{2.28}$$

The paraxial approximation consists in expanding the square root in 2.26 and retain only the second order terms in ϵ, assuming that $\epsilon \ll 1$. If we Taylor expand the square root we get:

$$\sqrt{k_0^2 - k_x^2 - k_z^2} = k_0\left[1 - \frac{k_x^2 + k_y^2}{k_0}\right]^{1/2} = k_0\left[1 - \frac{k_x^2 + k_y^2}{2k_0^2} + O(\epsilon^4)\right] \qquad (2.29)$$

A very natural scaling for the variables involved is the following, where the transverse coordinate x and y scale with w_0 and the longitudinal coordinate z scales with the Rayleigh length:

$$x' = \frac{x}{w_0}, \quad y' = \frac{y}{w_0}, \quad z' = \frac{z}{z_R}, \quad u_x = \frac{w_0 k_x}{2}, \quad u_y = \frac{w_0 k_y}{2}. \qquad (2.30)$$

By 2.30 and 2.29 the equation 2.26 takes the form:

$$\begin{aligned} E(x', y', z', t) =& \frac{1}{\pi}\int_{-\infty}^{+\infty} \mathrm{d}u_x\, \mathrm{d}u_y\, \exp\big[-(u_x^2 + u_y^2)\big] \\ & \exp\left\{ i\Big[2u_x x' + 2u_y y' + \frac{2z'}{\epsilon^2}\big(\sqrt{1 - \epsilon^2(u_x^2 + u_y^2)} - 1\big)\Big]\right\} e^{ik_0(z_R z' - ct)} \end{aligned} \qquad (2.31)$$

After the paraxial approximation the same equation reads:

$$\begin{aligned} E(x', y', z', t) =& \frac{1}{\pi}\int_{-\infty}^{+\infty} \mathrm{d}u_x\, \mathrm{d}u_y\, \exp\big[-(u_x^2 + u_y^2)\big] \\ & \exp\Big\{ i\big[2u_x x' + 2u_y y' - z'(u_x^2 + u_y^2)\big]\Big\} e^{ik_0(z_R z' - ct)} + O(\epsilon^2) \end{aligned} \qquad (2.32)$$

(note that in the phase $\exp(ik_0 z)$ there is z and not z'). This last integral is solvable in terms of Gaussian integrals. We can write the field E as:

$$E(x', y', z', t) = I(x')\, I(y')\, e^{ik_0(z_R z' - ct)}, \qquad (2.33)$$

where

$$I(x') = \frac{1}{\sqrt{\pi}}\int_{-\infty}^{+\infty} \mathrm{d}u_x\, \exp\left[-(1 + iz')\left(u_x^2 - \frac{2iu_x x'}{1 + iz'}\right)\right] \qquad (2.34)$$

$$= \frac{1}{\sqrt{\pi}}\int_{-\infty}^{+\infty} \mathrm{d}u_x\, \exp\left[-(1 + iz')\left(u_x - \frac{ix'}{1 + iz'}\right)^2\right] \exp\left(-\frac{x'^2}{1 + iz'}\right)$$

$$= \frac{1}{\sqrt{1 + iz'}}\, \exp\left(-\frac{x'^2}{1 + iz'}\right). \qquad (2.35)$$

From 2.33 we get:

$$E(x', y', z', t) = \frac{1}{1 + iz'} \exp\left(- \frac{x'^2 + y'^2}{1 + iz'} \right) e^{ik_0(z_R z' - ct)} \tag{2.36}$$

and after some algebraic passages we obtain the analytical expression of the monochromatic Gaussian pulse in paraxial approximation in the scaled variables 2.30:

$$E(x', y', z', t) = \frac{1}{w'(z')} \exp\left(-\frac{x'^2 + y'^2}{w'(z')^2}\right) \exp\left[i\left(z' \frac{x'^2 + y'^2}{w'(z')^2} - \delta\right)\right] e^{ik_0(z_R z' - ct)}, \tag{2.37}$$

where we defined

$$w'(z') = \sqrt{1 + z'^2}, \qquad \delta = \arctan(z'). \tag{2.38}$$

Non-scaled variables After having made the expansion 2.29 we can write the monochromatic Gaussian pulse in paraxial approximation without introducing the scaled variables:

$$E(x, y, z, t) = \frac{\pi w_0^2}{(2\pi)^2} \int_{-\infty}^{+\infty} \mathrm{d}k_x \, \mathrm{d}k_y \exp\left[- \frac{w_0^2}{4}(k_x^2 + k_y^2)\right] \exp\left[i\left(xk_x + yk_y - z\frac{k_x^2 + k_y^2}{2k_0}\right)\right] e^{ik_0(z - ct)}. \tag{2.39}$$

We can write the same field as:

$$E(x, y, z, t) = \pi w_0^2 \, I(x) \, I(y) \, e^{ik_0(z - ct)}, \tag{2.40}$$

where, if we define

$$\frac{1}{\sigma^2} = \frac{w_0^2}{2} + i\frac{z}{k_0} \tag{2.41}$$

the integrals above are given by:

$$I(x) = \frac{1}{2\pi} \int_{-\infty}^{+\infty} \mathrm{d}k_x \exp\left[- \frac{k_x^2}{2\sigma^2} + ik_x x\right] = \sqrt{\frac{\sigma^2}{2\pi}} \exp\left(- \frac{\sigma^2}{2} x^2\right). \tag{2.42}$$

The resulting expression for the field E is:

$$E(x, y, z, t) = \frac{w_0^2 \sigma^2}{2} \exp\left[- \frac{\sigma^2}{2}(x^2 + y^2)\right] e^{ik_0(z - ct)}. \tag{2.43}$$

In order to recover an expression equivalent to 2.37 we have to separate the real and imaginary part of σ^2. If we re-express σ in terms of the Rayleigh length 2.28 we find:

$$\frac{1}{\sigma^2} = \frac{w_0^2}{2} + iw_0^2\frac{z}{2z_R} = \frac{w_0^2}{2}\left(1 + i\frac{z}{z_R}\right) \tag{2.44}$$

Then we have:

$$\frac{\sigma^2}{2} = \frac{1}{w_0 w(z)}e^{-i\delta} = \frac{1}{w(z)^2}\left(1 - i\frac{z}{z_R}\right), \tag{2.45}$$

where we defined some quantities analogous to 2.38:

$$w(z) = w_0\sqrt{1 + \left(\frac{z}{z_R}\right)^2}, \qquad \delta = \arctan\left(\frac{z}{z_R}\right). \tag{2.46}$$

Thus the final expression for the filed E can be written:

$$E(x,y,z,t) = \frac{w_0}{w(z)}\,\exp\left(-\frac{x^2+y^2}{w(z)^2}\right)\exp\left[i\left(\frac{z}{z_R}\frac{x^2+y^2}{w(z)^2} - \delta\right)\right]e^{ik_0(z-ct)}. \tag{2.47}$$

As shown in 2.32, the paraxial approximation is correct for less than second order terms in ϵ.

2.2.2 Envelope equation for monochromatic pulse

Equation 2.47 can be re-written in compact form:

$$E(x,y,z,t) = E_0(x,y,z)\,e^{ik_0(z-ct)}. \tag{2.48}$$

E_0 satisfies the well-known Helmoltz equation

$$\frac{\partial^2 E_0}{\partial x^2} + \frac{\partial^2 E_0}{\partial y^2} + \frac{\partial^2 E_0}{\partial z^2} + 2ik_0\,\frac{\partial E_0}{\partial z} = 0, \tag{2.49}$$

and the following non-approximate expression for the field amplitude satisfies exactly the Helmoltz equation:

$$E_0(x,y,z;k_0) = \frac{1}{(2\pi)^2}\int_{-\infty}^{+\infty}\mathrm{d}k_x\,\mathrm{d}k_y\,\exp\left[-\frac{w_0^2}{4}(k_x^2+k_y^2)\right] \exp\left\{i\Big[xk_x + yk_y + z\Big(\sqrt{k_0^2-k_x^2-k_y^2} - k_0\Big)\Big]\right\}. \tag{2.50}$$

If we now perform the same scaling 2.30 for the variables x, y and z, the Helmoltz equation reads:

$$\frac{\partial^2 E_0}{\partial x'^2} + \frac{\partial^2 E_0}{\partial y'^2} + \epsilon^2 \frac{\partial^2 E_0}{\partial z'^2} + 4i \frac{\partial E_0}{\partial z'} = 0. \tag{2.51}$$

If $\epsilon \ll 1$ we can apply the paraxial approximation and neglect second order terms in ϵ. Turning back to the non-scaled original variables we get the envelope equation for the field amplitude E_0 in paraxial approximation

$$\frac{\partial^2 E_0}{\partial x^2} + \frac{\partial^2 E_0}{\partial y^2} + 2ik_0 \frac{\partial E_0}{\partial z} = 0, \tag{2.52}$$

in which the field amplitude E_0 in paraxial approximation given by 2.47 and 2.48 exactly fits:

$$\begin{aligned} E_0(x, y, z; k_0) = \frac{1}{(2\pi)^2} \int_{-\infty}^{+\infty} \mathrm{d}k_x \, \mathrm{d}k_y \, \exp\left[-\frac{w_0 4}{4}(k_x^2 + k_y^2) \right] \\ \exp\left[i\left(xk_x + yk_y - z\frac{k_x^2 + k_y^2}{2k_0} \right) \right] \\ = \frac{w_0}{w(z)} \exp\left[-\frac{x^2 + y^2}{w(z)^2} + i\Phi \right], \end{aligned} \tag{2.53}$$

where we have re-written the phase of E_0 as $\Phi = z(x^2 + y^2)/z_R w(z)^2 - \delta$.

2.2.3 Hermite-Gauss and Laguerre-Gauss modes

We have seen that the Gaussian pulse 2.47 is a solution of the paraxial Helmoltz equation 2.52. But 2.47 is only the lowest order of a more general solution. In fact, there exist many higher harmonics which contitute solution of the paraxial Helmoltz equation.

Depending on the nature of the problem, i.e. on the structure of the laser device involved, a detailed description of the beam can be made by taking the electromagnetic pulse to be a linear superposition of some suitable basis of functions $E_{a\,b}$:

$$E_{\mathrm{beam}} = \sum_{a,b} c_{ab} \tilde{E}_{ab}.$$

Hermite-Gauss modes If the problem one deals with has a rectangular symmetry the most suitable basis of function which can describe the pulse are the Hermite-Gauss modes. The basis function can be cast as:

$$\begin{aligned} E_{0,mn}(x, y, z, t, k_0) = \frac{w_0}{w(z)} H_m\left(\frac{\sqrt{2}x}{w(z)} \right) H_n\left(\frac{\sqrt{2}y}{w(z)} \right) \exp\left(-\frac{x^2 + y^2}{w(z)^2} \right) \\ \exp\left[i\left(\frac{z}{z_R} \frac{x^2 + y^2}{w(z)^2} - (m + n + 1)\delta \right) \right], \end{aligned} \tag{2.54}$$

where H are the hermite polynomials and are given by:

$$H_n(x) = (-1)^n \exp(x^2) \frac{d^n}{dx^n} \exp(-x^2). \tag{2.55}$$

Usually Hermite-Gauss modes are referred to as TEM_{mn} where m and n are the polynomial indices in the x and y direction (TEM stands for Transversal ElectroMagnetic). The lowest order Gaussian mode is typically referred to as TEM_{00}.

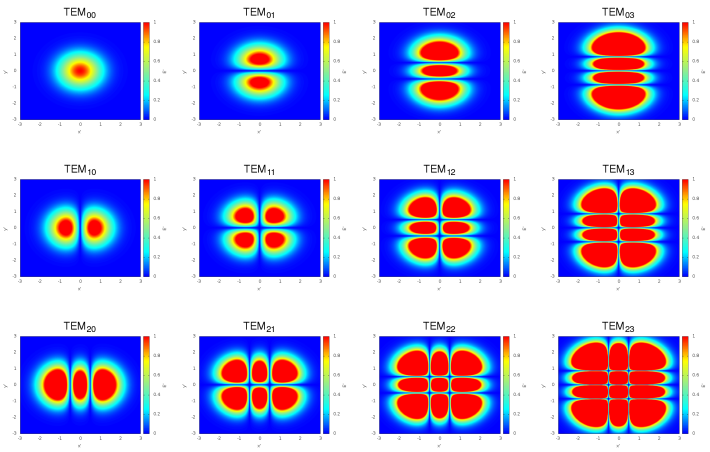

Figure 2.1: First Hermite-Gauss modes. There is represented the field in the transversal plane in $z = 0$. The polynomial indices are given in the titles of each plot. We see that the TEM_{00} mode is the usual Gaussian one.

Laguerre-Gauss modes If we are dealing with a beam which we know to have a cylindrical symmetry we would rather use the Laguerre-Gauss modes, given by:

$$E_{0,qp}(\rho, \phi, z, t, k_0) = \frac{w_0}{w(z)} \left(\frac{\sqrt{2}\rho}{w(z)} \right)^q L_q^p \left(\frac{\sqrt{2}\rho}{w(z)} \right) \exp\left(-\frac{\rho^2}{w(z)^2} \right) \exp\left[i \left(\frac{z}{z_R} \frac{\rho^2}{w(z)^2} - (2p + q + 1)\delta + iq\phi \right) \right], \tag{2.56}$$

where the generalized Laguerre polynomials L are given by Rodrigues' formula:

$$L_q^p(x) = \frac{x^{-p} e^x}{q!} \frac{d^q}{dx^q} (e^{-x} x^{q+p}). \tag{2.57}$$

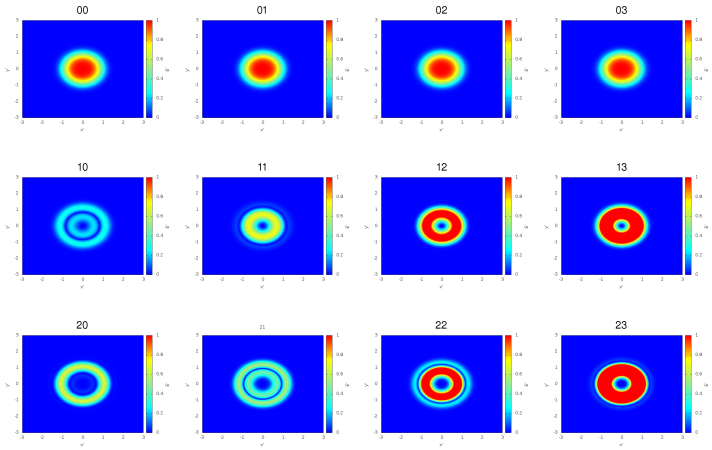

Figure 2.2: First Laguerre-Gauss modes.There is represented the field in the transversal plane in $z = 0$. The polynomial indices are given in the titles of each plot. We see that the 00 mode is the usual Gaussian one.

2.2.4 Monochromatic pulse exact solution

The integral 2.26 is not analytically solvable. Nevertheless we can evaluate it numerically or by means of infinite series. We can re-write this integral by introducing polar coordinates in the transversal plane xy:

$$x = r\cos\theta, \qquad y = r\sin\theta, \qquad k_x = K\cos\phi, \qquad k_y = K\sin\phi. \tag{2.58}$$

Thus the exact solution reads:

$$E(x,y,z,t;k_0) = \frac{\pi w_0^2}{(2\pi)^2}\int_0^\infty\int_0^{2\pi} \mathrm{d}K\,\mathrm{d}\phi\,K\,\exp\left[-\frac{w_0^2}{4}K^2\right] \exp\left[ik_0\left(z\sqrt{1-K^2/k_0^2}-ct\right)\right]\exp[iKr\cos(\phi-\theta)]. \tag{2.59}$$

Making use of the relation

$$e^{iz\cos\phi} = \sum_{n=-\infty}^{+\infty} i^n J_n(z)e^{ik\phi} \tag{2.60}$$

(where $J_n(z)$ are the Bessel functions of the first kind), we see that after the integration between 0 and 2π only the term of the series 2.60 with $n = 0$ does not vanish and the integral 2.59 becomes:

$$E(x,y,z,t;k_0) = \frac{w_0^2}{2}\int_0^\infty \mathrm{d}K\,K\,\exp\left[-\frac{w_0^2}{4}K^2\right] \exp\left[ik_0\left(z\sqrt{1-K^2/k_0^2}-ct\right)\right]J_0(Kr). \tag{2.61}$$

An alternative expression for the exact solution of the monochromatic pulse can be obtained by considering the following expansion:

$$\exp\left(ikz\sqrt{1-b^2}\right) = \left(\frac{\pi kz}{2}\right)^{1/2} \sum_{n=0}^{\infty} \frac{1}{n!}\left(\frac{kzb^2}{2}\right)^n H^{(1)}_{n-\frac{1}{2}}(kz), \tag{2.62}$$

with the $H^{(1)}_\nu$ indicating the Hankel functions (or Bessel functions of the third kind) given by $H^{(1)}_\nu(z) = J_\nu(z) + iN_\nu(z)$, where the J_ν and the N_ν are the first kind Bessel function and the second kind Bessel functions (sometimes called Neumann functions). By 2.61 and 2.62, setting $u = w_0K/2$, we get:

$$E(x,y,z,t;k_0) = 2e^{-i\omega_0 t}\left(\frac{\pi k_0 z}{2}\right)^{1/2} \sum_{n=0}^{\infty} \frac{1}{n!}\left(\frac{2z}{k_0 w_0^2}\right)^n H^{(1)}_{n-\frac{1}{2}}(k_0 z) \int_0^\infty \mathrm{d}u\, e^{-u^2}\, u^{2n+1}\, J_0\left(\frac{2}{w_0}ur\right). \tag{2.63}$$

Using the relation (valid for $n \in \mathbf{N} \cup \{0\}$ and $(n + \mathrm{Re}\mu) > -1$)

$$\int_0^\infty \mathrm{d}x\, e^{-x^2}\, x^{2n+\mu+1}\, J_\mu(2x\sqrt{z}) = \frac{n!}{2} e^{-z} z^{\mu/2} L^\mu_n(z) \tag{2.64}$$

(where the L^μ_n are the generalized Laguerre polynomials and L^0_n is the n-*th* Laguerre polynomial)we find the exact expression of the monochromatic pulse in the form of an infinite series:

$$E(x,y,z,t;k_0) = e^{-i\omega_0 t}\left(\frac{\pi k_0 z}{2}\right)^{1/2} \sum_{n=0}^{\infty} \left(\frac{z}{z_R}\right)^n \exp\left(-\frac{x^2+y^2}{w_0^2}\right) H^{(1)}_{n-\frac{1}{2}}(k_0 z)\, L^0_n\left(\frac{x^2+y^2}{w_0^2}\right). \tag{2.65}$$

2.2.5 Components of the electromagnetic field

As we have said at the beginning of the chapter, in all the calculations above E could represent any of the component of **E**, **B** or **A**. Now we want to derive the six cartesian components of the electomagnetic field of a monochromatic pulse. In order to do this we use Maxwell's equations 2.1a and 2.1b without sources in vacuum, which we recall below:

$$\nabla \cdot \mathbf{E} = 0$$
$$\nabla \times \mathbf{E} = -\frac{1}{c}\frac{\partial \mathbf{B}}{\partial t}$$

Because there is one equation (the divergence one) for three variables, in order to determine the three components of the electric field we have to fix two of them. Some authors fix E_x and put $E_y = 0$ and then they find E_z. We prefer to fix E_x and E_y so that they differs only for the amplitude and then we find E_z. The three components of the magnetic field will be derived by making use of the equation for the curl of $\mathbf{E}$.

We have just seen that if we make the choice $\hat{E}(k_x, k_y, k_z) \propto \exp[-w_0^2(k_x^2 + k_y^2)/4]$ as in 2.26 we obtain an expression for the field E in paraxial approximation given by 2.47. From 2.47 we see that $E(x, y, 0, 0) = \exp[-(x^2+y^2)/w_0^2]$. So we can fix E_x and E_y in the conditions $z = 0, t = 0$ for less than the amplitude:

$$E_x(x, y, 0, 0) = E_{0x} \exp\left(- \frac{x^2 + y^2}{w_0^2} \right), \tag{2.66a}$$

$$E_y(x, y, 0, 0) = E_{0y} \exp\left(- \frac{x^2 + y^2}{w_0^2} \right). \tag{2.66b}$$

If $\Theta(x, y, z) = xk_x + yk_y + z\sqrt{k_0^2 - k_x^2 - k_y^2}$, we can write the exact integral solution of the wave equation for E_x and E_y, to which we will apply the paraxial approximation again:

$$E_x(x, y, z, t; k_0) = \frac{\pi w_0^2}{(2\pi)^2} \int_{-\infty}^{+\infty} \mathrm{d}k_x \, \mathrm{d}k_y \, E_{0x} \exp\left[- \frac{w_0^2}{4}(k_x^2 + k_y^2) \right] \exp\left[i\Big(\Theta - \omega_0 t \Big) \right] \tag{2.67}$$

$$E_y(x, y, z, t; k_0) = \frac{\pi w_0^2}{(2\pi)^2} \int_{-\infty}^{+\infty} \mathrm{d}k_x \, \mathrm{d}k_y \, E_{0y} \exp\left[- \frac{w_0^2}{4}(k_x^2 + k_y^2) \right] \exp\left[i\Big(\Theta - \omega_0 t \Big) \right]. \tag{2.68}$$

We avoid to solve right now these integral in paraxial approximation and then derive E_z from the divergence equation. If we did that we would find a very complicated expression for E_z since it is given by:

$$E_z = - \int^z \mathrm{d}z' \left(\frac{\partial E_x}{\partial x} + \frac{\partial E_y}{\partial y} \right). \tag{2.69}$$

Using the divergence equation with 2.67 and 2.68 we get the integral expression for E_z:

$$E_z(x, y, z, t; k_0) = - \frac{\pi w_0^2}{(2\pi)^2} \int_{-\infty}^{+\infty} \mathrm{d}k_x \, \mathrm{d}k_y \, \frac{k_x E_{0x} + k_y E_{0y}}{\sqrt{k_0^2 - k_x^2 - k_y^2}} \exp\left[- \frac{w_0^2}{4}(k_x^2 + k_y^2) \right] \exp\left[i\Big(\Theta - \omega_0 t \Big) \right] \tag{2.70}$$

Assuming that from a monochromatic pulse $\mathbf{E} = \mathbf{E}_0 e^{-i\omega_0 t}$ the magnetic field is in the form $\mathbf{B} = \mathbf{B}_0 e^{-i\omega_0 t}$, from the equation for the curl of $\mathbf{E}$ we get:

$$\mathbf{B} = \frac{c}{i\omega_0}\nabla \times \mathbf{E}. \tag{2.71}$$

Thus the components of the magnetic field are given by three integral expressions:

$$B_x(x,y,z,t;k_0) = -\frac{1}{k_0}\frac{\pi w_0^2}{(2\pi)^2}\int_{-\infty}^{+\infty} \mathrm{d}k_x\,\mathrm{d}k_y\,\frac{k_x k_y E_{0x} + (k_0^2 - k_x^2)E_{0y}}{\sqrt{k_0^2 - k_x^2 - k_y^2}} \exp\Big[-\frac{w_0^2}{4}(k_x^2+k_y^2)\Big]\exp\Big[i\Big(\Theta - \omega_0 t\Big)\Big] \tag{2.72}$$

$$B_y(x,y,z,t;k_0) = \frac{1}{k_0}\frac{\pi w_0^2}{(2\pi)^2}\int_{-\infty}^{+\infty} \mathrm{d}k_x\,\mathrm{d}k_y\,\frac{(k_0^2 - k_y^2)E_{0x} + k_x k_y E_{0y}}{\sqrt{k_0^2 - k_x^2 - k_y^2}} \exp\Big[-\frac{w_0^2}{4}(k_x^2+k_y^2)\Big]\exp\Big[i\Big(\Theta - \omega_0 t\Big)\Big] \tag{2.73}$$

$$B_z(x,y,z,t;k_0) = \frac{1}{k_0}\frac{\pi w_0^2}{(2\pi)^2}\int_{-\infty}^{+\infty} \mathrm{d}k_x\,\mathrm{d}k_y\,(k_x E_{0y} - k_y E_{0x}) \exp\Big[-\frac{w_0^2}{4}(k_x^2+k_y^2)\Big]\exp\Big[i\Big(\Theta - \omega_0 t\Big)\Big]. \tag{2.74}$$

If we now perform the paraxial approximation we will see that each one of the components of the electromagnetic field can be cast as a sum $E = \sum_k c_k I_m(x) I_n(y)$, with $m, n \in \{1,2,3,4\}$. The integrals I_m are given by:

$$I_m(x) = \frac{1}{2\pi}\int_{-\infty}^{+\infty} \mathrm{d}k_x\,\exp\Big[-\frac{w_0^2}{4}k_x^2 + i\Big(-\frac{z}{2k_0}k_x^2 + x k_x\Big)\Big]k_x^m. \tag{2.75}$$

Using 2.41 and making the change of variable $k'_x = k_x - i\sigma^2 x$ we get:

$$I_m(x) = \frac{1}{2\pi}\exp\Big(-\frac{\sigma^2}{2}x^2\Big)\int_{-\infty}^{+\infty}\mathrm{d}k'_x\exp\Big(-\frac{k_x'^2}{2\sigma^2}\Big)(k'_x + i\sigma^2 x)^m \tag{2.76}$$

The result of this integral derives in turn from another kind of integral:

$$K_s = \frac{1}{2\pi}\int_{-\infty}^{+\infty}\mathrm{d}k'_x\,\exp\Big(-\frac{k_x'^2}{2\sigma^2}\Big)k_x'^s = \frac{1}{2\pi}\sqrt{2\sigma^2}(2\sigma^2)^{s/2}\int_{-\infty}^{+\infty}\mathrm{d}u\,e^{-u^2}u^s. \tag{2.77}$$

When s is odd the K_s vanish, while when s is even the K_s are calculated deriving the raltion $\int_{-\infty}^{+\infty} \mathrm{d}u\, e^{-\alpha u^2}$ with respect to α and then setting $\alpha = 1$. Then The K_s ($s \leq 4$)are given by:

$$K_0 = \sqrt{\frac{\sigma^2}{2\pi}}, \quad K_1 = 0, \quad K_2 = \sigma^2\sqrt{\frac{\sigma^2}{2\pi}}, \quad K_3 = 0, \quad K_4 = 3\sigma^4\sqrt{\frac{\sigma^2}{2\pi}}. \quad (2.78)$$

Since the I_m can be written in terms of the K_s in a simple way, thw final result for the integrals I_m is:

$$\begin{aligned}
I_0(x) &= e^{-\sigma^2x^2/2}\sqrt{\frac{\sigma^2}{2\pi}}, \\
I_1(x) &= ix\sigma^2 e^{-\sigma^2x^2/2}\sqrt{\frac{\sigma^2}{2\pi}}, \\
I_2(x) &= (\sigma^2 - \sigma^4x^2)e^{-\sigma^2x^2/2}\sqrt{\frac{\sigma^2}{2\pi}} \\
I_3(x) &= (3i\sigma^4x - i\sigma^6x^3)e^{-\sigma^2x^2/2}\sqrt{\frac{\sigma^2}{2\pi}}, \\
I_4(x) &= (3\sigma^4 - 6\sigma^6x^2 + \sigma^8x^4)e^{-\sigma^2x^2/2}\sqrt{\frac{\sigma^2}{2\pi}}
\end{aligned} \quad (2.79)$$

Now we give the expressions of the six components of the fields in terms of the I_m:

$$E_x(x,y,z,t;k_0) = \pi w_0^2 E_{0x} I_0(x) I_0(y) e^{ik_0(z-ct)} \quad (2.80a)$$

$$E_y(x,y,z,t;k_0) = \pi w_0^2 E_{0y} I_0(x) I_0(y) e^{ik_0(z-ct)} \quad (2.80b)$$

$$\begin{aligned}
E_z(x,y,z,t;k_0) = -\pi w_0 \Bigg\{ & E_{0x}\left[\frac{I_1(x)I_0(y)}{k_0} + \frac{I_3(x)I_0(y)}{2k_0^3} + \frac{I_1(x)I_2(y)}{2k_0^3}\right] + \\
& + E_{0y}\left[\frac{I_0(x)I_1(y)}{k_0} + \frac{I_2(x)I_1(y)}{2k_0^3} + \frac{I_0(x)I_3(y)}{2k_0^3}\right]\Bigg\}
\end{aligned} \quad (2.80c)$$

(2.80d)

$$B_x(x,y,z,t;k_0) = -\pi w_0^2\Bigg\{E_{0x}\left[\frac{I_1(x)I_1(y)}{k_0^2} + \frac{I_3(x)I_1(y)}{2k_0^4} + \frac{I_1(x)I_3(y)}{2k_0^4}\right] + \\ + E_{0y}\Bigg[I_0(x)I_0(y) + \frac{I_2(x)I_0(y)}{2k_0^2} + \frac{I_0(x)I_2(y)}{2k_0^2} + \\ - \frac{I_2(x)I_0(y)}{k_0^2} - \frac{I_4(x)I_0(y)}{2k_0^4} - \frac{I_2(x)I_2(y)}{2k_0^4}\Bigg]\Bigg\} \tag{2.81a}$$

$$B_y(x,y,z,t;k_0) = \pi w_0^2\Bigg\{E_{0x}\Bigg[I_0(x)I_0(y) + \frac{I_2(x)I_0(y)}{2k_0^2} + \frac{I_0(x)I_2(y)}{2k_0^2} + \\ - \frac{I_0(x)I_2(y)}{k_0^2} - \frac{I_2(x)I_2(y)}{2k_0^4} - \frac{I_0(x)I_4(y)}{2k_0^4}\Bigg] + \\ E_{0y}\left[\frac{I_1(x)I_1(y)}{k_0^2} + \frac{I_3(x)I_1(y)}{2k_0^4} + \frac{I_1(x)I_3(y)}{2k_0^4}\right]\Bigg\} \tag{2.81b}$$

$$B_z(x,y,z,t;k_0) = \pi w_0^2\left[E_{0x}\frac{I_1(x)I_0(y)}{k_0} - E_{0y}\frac{I_0(x)I_1(y)}{k_0}\right]. \tag{2.81c}$$

Using 2.79 we obtain the six components of the electromagnetic field in function of the parameter $\sigma^2 = (w_0^2/2 + iz/k_0)^{-1}$. If we call $\Lambda = (w_0/w)\exp[-(x^2 + y^2)/w^2]$ and $\Psi = z(x^2+y^2)/z_R w(z) - \delta + k_0(z-ct)$ we recover the expression 2.47 of the monochromatic pulse in paraxial approximation for E_x and E_y.

$$E_x(x,y,z,t;k_0) = E_{0x}\Lambda\exp(i\Psi) \tag{2.82a}$$

$$E_y(x,y,z,t;k_0) = E_{0y}\Lambda\exp(i\Psi) \tag{2.82b}$$

$$E_z(x,y,z,t;k_0) = -\Bigg\{E_{0x}\left[\frac{i\sigma^2}{k_0}x + \frac{ix\sigma^4}{2k_0^3}(3 - x^2\sigma^2) + \frac{ix\sigma^4}{2k_0^3}(1 - y^2\sigma^2)\right] + \\ + E_{0y}\left[\frac{i\sigma^2}{k_0}y + \frac{iy\sigma^4}{2k_0^3}(1 - x^2\sigma^2) + \frac{iy\sigma^4}{2k_0^3}(3 - y^2\sigma^2)\right]\Bigg\}\Lambda\exp(i\Psi) \tag{2.82c}$$

$$B_x(x,y,z,t;k_0) = \Bigg\{E_{0x}\left[+ \frac{xy\sigma^4}{k_0^2} + \frac{xy\sigma^6}{2k_0^4}(3 - x^2\sigma^2) + \frac{xy\sigma^6}{2k_0^4}(3 - y^2\sigma^2)\right] + \\ - E_{0y}\Bigg[1 + \frac{\sigma^2}{2k_0^2}(1 - x^2\sigma^2) + \frac{\sigma^2}{2k_0^2}(1 - y^2\sigma^2) - \frac{\sigma^2}{k_0^2}(1 - x^2\sigma^2) + \\ - \frac{\sigma^4}{2k_0^4}(x^4\sigma^4 - 6x^2\sigma^2 + 3) + \\ - \frac{\sigma^4}{2k_0^4}(x^2y^2\sigma^4 - x^2\sigma^2 - y^2\sigma^2 + 1)\Bigg]\Bigg\}\Lambda\exp(i\Psi) \tag{2.82d}$$

$$B_y(x,y,z,t;k_0) = -\Big\{ E_{0y}\Big[+ \frac{xy\sigma^4}{k_0^2} + \frac{xy\sigma^6}{2k_0^4}(3-x^2\sigma^2) + \frac{xy\sigma^6}{2k_0^4}(3-y^2\sigma^2)\Big] + \\ - E_{0x}\Big[1 + \frac{\sigma^2}{2k_0^2}(1-x^2\sigma^2) + \frac{\sigma^2}{2k_0^2}(1-y^2\sigma^2) - \frac{\sigma^2}{k_0^2}(1-y^2\sigma^2) + \\ - \frac{\sigma^4}{2k_0^4}(y^4\sigma^4 - 6y^2\sigma^2 + 3) + \\ - \frac{\sigma^4}{2k_0^4}(x^2y^2\sigma^4 - x^2\sigma^2 - y^2\sigma^2 + 1)\Big]\Big\}\,\Lambda\exp(i\Psi) \quad (2.82e)$$

$$B_z(x,y,z,t;k_0) = \frac{i\sigma^2}{k_0}\big[E_{0x}x - E_{0y}y\big]\,\Lambda\exp(i\Psi). \quad (2.82f)$$

2.3 Finite pulse

If we want our electromagnetic pulse to be longitudinally shaped with a rapidly decreasing or compactly supported function $f(z)$ we make the choice:

$$\hat{E}_{\text{fin}}(k_x,k_y,k_z) = \exp\Big[-\frac{w_0^2}{4}(k_x^2+k_y^2)\Big]\,\hat{f}(k_z-k_0), \quad (2.83)$$

where, for instance, f is Gaussian:

$$f(z) = \exp\Big(-\frac{z^2}{w_z^2}\Big), \qquad \hat{f}(k_z-k_0) = \exp\Big[-\frac{w_z^2}{4}(k_Z-k_0)^2\Big]. \quad (2.84)$$

In this case we have that the field amplitude significantly differs from 0 for $|z| \le w_z$ and a characteristic time which gives the order of magnitude of the pulse duration is given by:

$$\tau = \frac{2w_z}{c}. \quad (2.85)$$

If we had a one-dimensionale wave we would obtain a length-modulated pulse:

$$E_{\text{fin}}(z,t) = \frac{1}{2\pi}\int_{-\infty}^{+\infty} \mathrm{d}k_z\ \exp[ik_z(z-ct)]\hat{f}(k_z-k_0)$$

$$= \frac{1}{2\pi}\exp[ik_0(z-ct)]\int_{-\infty}^{+\infty}\mathrm{d}k_z'\ \exp[ik_z'(z-ct)]\hat{f}(k_z')$$

$$= f(z-ct)\ \exp[ik_0(z-ct)]. \quad (2.86)$$

However in our treatise we do not deal with one-domensional wave. If we have

the more general expression 2.83 we have to use 2.11 again (Θ is defined in the previous section):

$$E_{\rm fin}(x,y,z,t) = \frac{1}{(2\pi)^3}\int_{-\infty}^{+\infty} {\rm d}k_x\,{\rm d}k_y\,\hat{E}(k_x,k_y,k_z)\exp\left[i\Big(\Theta-\omega_0 t\Big)\right]$$

$$= \frac{1}{2\pi}\int_{-\infty}^{+\infty} {\rm d}k_z\,\hat{f}(k_z-k_0)\left\{\frac{1}{(2\pi)^2}\iint_{-\infty}^{+\infty}{\rm d}k_x\,{\rm d}k_y\,\exp\left[-\frac{w_0^2}{4}(k_x^2+k_y^2)\right]\right.$$
$$\left.\exp\left[i\Big(\Theta-\omega_0 t\Big)\right]\right\}$$

$$= \frac{1}{2\pi}\int_{-\infty}^{+\infty} {\rm d}k_z\,\hat{f}(k_z-k_0)\,E_{\rm mc}(x,y,z,t;k_z). \qquad (2.87)$$

The last expression gives the implicit solution of the finite pulse case. $E_{\rm mc}$ is the expression, either exact or in paraxial approximation, of the monochromatic pulse of frequency $\omega = ck_z$. If we write it as $E_{\rm mc} = E_0(x,y,z,t;k_z)\exp[ik_z(z-ct)]$ the finite pulse solution reads:

$$E_{\rm fin}(x,y,z,t) = \frac{1}{2\pi}\int_{-\infty}^{+\infty} {\rm d}k_z\,E_0(x,y,z,t;k_z)\exp[ik_z(z-ct)]\,\hat{f}(k_z-k_0). \quad (2.88)$$

If the $\hat{f}(k_z-k_0)$ is sufficiently peaked in k_0 we can evaluate E_0 in k_0 and take it out of the integral sign. Thus 2.86 leads to the final approximate result:

$$E_{\rm fin}(x,y,z,t;k_0) = E_0(x,y,z,t;k_0)\,f(z-ct)\,\exp[ik_0(z-ct)]. \qquad (2.89)$$

2.3.1 Envelope equation for finite pulse

We want now which equations E_0 obeys. For this purpose we apply the wave equation 2.7 to 2.89 finding:

$$\frac{\partial^2 E_0}{\partial x^2}+\frac{\partial^2 E_0}{\partial y^2}+2ik_0\frac{\partial E_0}{\partial z}+\frac{\partial^2 E_0}{\partial z^2}+2\frac{\partial E_0}{\partial z}\frac{\partial \log f}{\partial z}=0. \qquad (2.90)$$

We want to evaluate the last two terms. If we assume that f is Gaussian, i.e. $f(z)=\exp(-z^2/w_z^2)$ we have that $\partial\log f/\partial z = f'(z)/f(z) = -2z/w_z^2$ and making the scaling 2.30 we obtain:

$$\frac{\partial^2 E_0}{\partial x'^2}+\frac{\partial^2 E_0}{\partial y'^2}+4i\frac{\partial E_0}{\partial z}+\epsilon^2\frac{\partial^2 E_0}{\partial z^2}-4\frac{w_0^2}{w_z^2}z'\frac{\partial E_0}{\partial z}=0. \qquad (2.91)$$

In paraxial approximation ($\epsilon = w_0/z_R \ll 1$) the $O(\epsilon^2)$ terms can be neglected.

Moreover for $\hat{f}(k_z - k_0)$ to be sharply peaked around k_0 the longitudinal waist w_z must be very large ($w_z \gg w_0$). In order to neglect the last term we also require $\epsilon = w_0/z_R$ and w_0/w_z to be of the same order, so that the further condition $w_z \geq z_R$ must be added. In these condition the last two terms of 2.91 can be both neglected and turning back to the non-scaled variables we get the same paraxial Helmoltz equation found before (equation 2.52):

$$\frac{\partial^2 E_0}{\partial x^2} + \frac{\partial^2 E_0}{\partial y^2} + 2ik_0 \frac{\partial E_0}{\partial z} = 0. \tag{2.92}$$

If the condition $w_z \gg w_0$ is not strictly satisfies and the pulse has a shorter duration τ we can build a correction by expanding the finite pulse around k_0:

$$E_0(x, y, z, t; k_z) = E_0(x, y, z, t; k_0) + (k_z - k_0)\frac{\partial E_0}{\partial k_z}(x, y, z, t; k_z). \tag{2.93}$$

If we substitute 2.93 in 2.88 we get:

$$\begin{aligned} E(x, y, z, t) = \frac{1}{2\pi} e^{ik_0(z-ct)} \int_{-\infty}^{+\infty} \mathrm{d}k_z \exp\left[i\,(k_z - k_0)(z - ct)\right] \hat{f}(k_z - k_0) \\ \left[E_0(x, y, z, t; k_0) + (k_z - k_0)\frac{\partial E_0}{\partial k_z}(x, y, z, t; k_z)\right] \end{aligned}$$

$$\begin{aligned} = E_0(x, y, z, t; k_0)\, f(z - ct)\, \exp[ik_0(z - ct)] \\ - i\frac{\partial E_0}{\partial k_z}(x, y, z, t; k_0)\, f'(z - ct)\, \exp[ik_0(z - ct)], \end{aligned} \tag{2.94}$$

where the derivation of f is meant to be with respect to $(z - ct)$ and where we used the relation (with $\bar{\mathcal{F}}$ indicating the inverse Fourier transform):

$$\frac{\mathrm{d}^\alpha}{\mathrm{d}z^\alpha}\left(\bar{\mathcal{F}} f(k)\right) = \bar{\mathcal{F}}\left[(ik)^\alpha f(k)\right]. \tag{2.95}$$

Chapter 3

Analysis of the pulses

So far we have obtained the expressions for one of the component of the electromagnetic field in the case of a monochromatic wave of frequency $\omega_0 = ck_0$ and for a wave longitudinally shaped by a function $f(z)$.

In the first case we can have the exact solution in an integral or infinite-series form, but we get also an analytical expression for the monochromatic pulse by assuming the condition $\epsilon = w_0/z_R$ holds, so performing the paraxial approximation. By taking as initial conditions the 2.66 we have obtained all the components of the fields $\mathbf{E}$ and $\mathbf{B}$ by solving Maxwell's equations.

If the monochromatic pulse get shaped by a rapidly decreasing or compactly supported function the pulse is no longer monochromatic. In this case we found the integral expression 2.88, which is already an approximate solution (from the usual paraxial approximation). In order to obtain the analytical expression 2.89 we made another approximation, i.e., we evaluate $k_z = k_0$ if the $\hat{f}(k_z - k_0)$ is sufficiently peaked in k_0. Then 2.89 suffers from two approximations.

In this chapter we initially give some useful parameters which characterize different pulses, like the curvature radius, the beam divergence, the Gouy phase, and some temporal parameters which characterizes the duration of the pulses.

We have chose two representative examples of rapidly decreasing or compactly supported function. We recall now that a function is rapidly decreasing if and only if it belongs to the Schwartz space. In one dimension, a function $f(z)$ is said to be rapidly decreasing if and only if $f \in C^\infty(\mathbb{R})$ and

$$\sup_{z\in\mathbb{R}} |x^\alpha f^{(\beta)}(z)| < \infty,$$

with $\alpha, \beta \in \mathbb{N}$. This means that f is extremely regular and for $z \to \pm\infty$ it goes to zero more quickly than any power function. The classic example of rapidly decresing function is the Gaussian (we give here also its Fourier transform):

$$f(z) = \exp\left(-\frac{z^2}{w_z^2}\right), \qquad \hat{f}(k_z) = w_0\sqrt{\pi}\,\exp\left(-\frac{w_0^2}{4}k_z^2\right) \tag{3.1}$$

A function is compactly supported if the closure of the set $S = \{z :\ f(z) \neq 0\}$

is a compact set. A representative compactly supported function is:

$$f(z) = \begin{cases} \cos^2(\pi z/2w_z), & |z| < w_z \\ 0, & \text{elsewhere} \end{cases}, \qquad \hat{f}(k_z) = \frac{\pi^2}{\pi^2 - k_z^2 w_z^2} \frac{\sin(k_z w_z)}{k_z} \tag{3.2}$$

We have chose $\cos^2$ in order to have a C^1 function; if we had chose for example a cos function it would have been only C^0. In Figure 3.1(a) - 3.1(d) we give the trends of these functions.

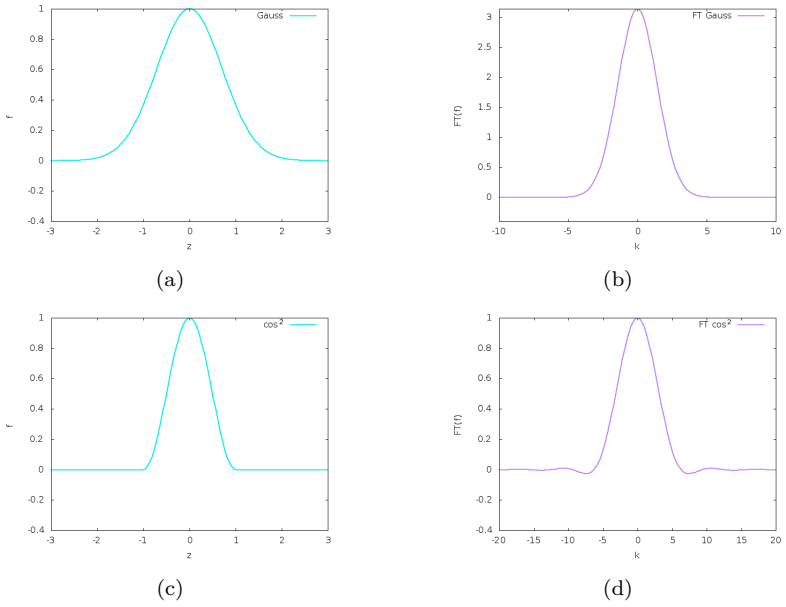

(a) (b) (c) (d)

Figure 3.1: Left: graphs of the Gaussian function (rapidly decreasing) and the $\cos^2$ function (complactly supported). Right: Fourier transform of the Gaussian function and the $\cos^2$ function. In the definitions 3.1 and 3.2 we have set $w_z = 1$.

3.1 Pulse parameters

The expressions we refer to in the following paragraphs are essentially the monocromatic pulses in scaled and non-scaled variables 2.47 and 2.37. We express all the parameters either in the scaled and non-scaled variables.

Spacial parameters We can characterize the beam spacial extension by some measures which deal with its transversal and longitudinal dimensions.

We take the quantity

$$w(z) = w_0 \left[1 + \left(\frac{z}{z_R} \right)^2 \right]^{1/2} = (1 + z'^2)^{1/2} = w'(z')$$

as the transversal beam parameter. Physically this quantity represents the

distance $\rho = (x^2 + y^2)^{1/2}$ at which the numerical value of the field reduces of the factor e^{-1}, for fixed z. $w(z)$ then characterizes the transversal beam width all along its longitudinal exptension.

If se settle in the focus $z = 0$ we can define the HWHM (Half Width Half Maximum) and FWHM (Full Width Half Maximum) waists, respectively $w_{\,\mathrm{HWHM}}$ and $w_{\,\mathrm{FWHM}}$. At the focus the instensity is given by:

$$I = |E(\rho, 0, 0)|^2 = I_0 \exp(-2\rho^2/w_0^2), \tag{3.3}$$

where I_0 is the intensity for $\rho = 0$ ($I_0 = 1$ for the monochromatic pulse in paraxial approximation but, in general, $I_0 \neq 1$). The HWHM waist is defined by the property:

$$I(w_{\,\mathrm{HWHM}}) = I_0/2. \tag{3.4}$$

Defining $w_{\,\mathrm{FWHM}} = 2\, w_{\,\mathrm{HWHM}}$ we get:

$$w_{\,\mathrm{HWHM}} = w_0 \sqrt{\frac{\log 2}{2}} \approx 0,59\, w_0 \tag{3.5a}$$

$$w_{\,\mathrm{FWHM}} = w_0 \sqrt{2\, \log 2} \approx 1,18\, w_0. \tag{3.5b}$$

In order to get a longitudinal measure for the beam we define the intensity in the focus axis:

$$I(z) = |E(0, z, 0)|^2. \tag{3.6}$$

In the case of the Gaussian and the $\cos^2$ functions it is given respectively by:

$$I(z) = I_0' \cos^4(\pi z/2w_z) \tag{3.7a}$$

$$I(z) = I_0' \exp(-2z^2/w_z^2) \tag{3.7b}$$

We define the HWHM length $L_{\,\mathrm{HWHM}}$ by the equality:

$$I(L_{\,\mathrm{HWHM}}) = I_0'/2. \tag{3.8}$$

Thus for the Gaussian and the $\cos^2$ functions $L_{\,\mathrm{HWHM}}$ is given respectively by:

$$L_{\,\mathrm{HWHM}} = 0,589\, w_z \tag{3.9a}$$

$$L_{\,\mathrm{HWHM}} = 0,364\, w_z. \tag{3.9b}$$

Beam divergence We note that the expression of $w(z)$ (or the $w'(z')$ one) draws an hyperbola in the plane $w(z)\,z$:

$$\frac{w(z)^2}{w_0^2} - \frac{z^2}{z_R^2} = 1 \tag{3.10a}$$

$$w'(z')^2 - z'^2 = 1. \tag{3.10b}$$

If we set $z = z' = 0$ we see that $w(z) = w_0$, which is a minimum for $w(z)$. In physical terms this can be interpreted by saying that the beam is focused in $z = 0$. If we search for the asymptotes of the hyperbole 3.10a and 3.10b we see that the beam has a well-defined divergence. Being the asymptotes given by:

$$w(z) = \frac{w_0}{z_R} z \tag{3.11a}$$

$$w'(z') = z'. \tag{3.11b}$$

The slope of the linear functions 3.11a and 3.11b gives the tangent of the angle which characterizes the beam divergence:

$$\tan\theta = \frac{w_0}{z_R} = \frac{2}{k_0 w_0} = \frac{\lambda_0}{\pi w_0} = \epsilon. \tag{3.12}$$

If the paraxial approximation can be hold as valid we can state:

$$\theta = \epsilon + O(\epsilon^3). \tag{3.13}$$

Curvature radius In literature it is often introduced the curvature radius of the wave fronts. The expression which we will get is valid for $z \gg z_R$. The surfaces of constant phase are given by:

$$\rho'^2 \frac{z'}{w'(z')^2} + k_0 z_R z' - k_0 z_R C' = 0 \tag{3.14a}$$

$$\rho^2 \frac{z}{w(z)^2} + k_0 z_R z - k_0 z_R C = 0, \tag{3.14b}$$

where $\rho' = \rho/w_0$ and C, C' are some constants. $\delta = \arctan(z/z_R)$ has not been included in the definition of the constant phase surfaces because, as $z \to \pm\infty$, $\delta \to \pm\pi/2$ and it can be included in the constant C. Equations 3.14a and 3.14b can be written in the form:

$$z'(\rho') = -\alpha' \rho'^2 + C' \tag{3.15a}$$

$$z(\rho) = -\alpha \rho^2 + C, \tag{3.15b}$$

where $\alpha' = z'/w'(z')^2 k_0 z_R$ and, analogously, $\alpha = z/w(z)^2 k_0 z_R$. For $z \to \pm\infty$ we have that $\alpha \to \pm 0$. Moreover, if the condition $z \gg z_R$ we can consider the approximation $\alpha = \text{const}$. In fact, if this last condition holds, from the equivalence $(1+x^2)^{1/2} = x + O(1/x)$ for $x \to \infty$, we have:

$$\alpha'(z') = \frac{1}{k_0 z_R}\frac{z'}{1+z'^2} = \frac{1}{k_0 z_R}\frac{1/z'}{1+O(1/z'^2)} = \frac{1}{k_0 z_R}\frac{1}{z'}\left[1+O\big(1/z'^2\big)+O\big(1/z'^4\big)\right] \tag{3.16a}$$

$$\alpha(z) = \frac{1}{k_0 w_0^2}\frac{z/z_R}{\left[1+(z/z_R)^2\right]} = \frac{1}{k_0 w_0^2}\frac{z_R}{z}\left[1+O\big(z_R^2/z^2\big)+O\big(z_R^4/z^4\big)\right]. \tag{3.16b}$$

This if $z' \gg 1$, i.e. $z \gg z_R$, α experiences little variations and can be considered constant. In general, if we have a function $y = f(x)$ the curvature radius is given by $R(x) = (1+y'^2)^{3/2}/|y''|$ and, for $y' \ll 1$ the curvature radius is $R(x) \approx |y''(x)|$. Note that they are positive quantities, as a radius must be. Using these formulae, we get:

$$R'(\rho') = \frac{(1+4\alpha'^2\rho'^2)^{3/2}}{2|\alpha'|} \tag{3.17a}$$

$$R(\rho) = \frac{(1+4\alpha^2\rho^2)^{3/2}}{2|\alpha|}, \tag{3.17b}$$

and, if we settle in the focal axis $\rho = \rho' = 0$, we get:

$$R'(0) = \frac{1}{2|\alpha'|} = \frac{k_0 z_R}{2}\frac{1+z'^2}{|z'|} \tag{3.18a}$$

$$R(0) = \frac{1}{2|\alpha|} = \frac{z_R^2}{|z|}\left[1+\left(\frac{z}{z_R}\right)^2\right] \tag{3.18b}$$

If we now define the signed curvature radii as follows:

$$\begin{aligned}\mathcal{R}' &= R'(0)\ \text{sgn}(z')\\ \mathcal{R} &= R(0)\ \text{sgn}(z),\end{aligned} \tag{3.19}$$

we can re-write 2.37 and 2.47 as:

$$E(x',y',z',t) = \frac{1}{w'(z')} \exp\left(- \frac{x'^2 + y'^2}{w'(z')^2} \right) \exp\left[i \frac{k_0 z_R}{2} \left(\frac{x'^2 + y'^2}{\mathcal{R}'} - \delta \right) \right] e^{ik_0(z_R z' - ct)} \tag{3.20a}$$

$$E(x,y,z,t) = \frac{w_0}{w(z)} \exp\left(- \frac{x^2 + y^2}{w(z)^2} \right) \exp\left[i \left(k_0 \frac{x^2 + y^2}{2\mathcal{R}} - \delta \right) \right] e^{ik_0(z - ct)} \tag{3.20b}$$

Gouy phase The Gouy phase is defined by:

$$\delta(z) = \arctan\left(\frac{z}{z_R} \right)$$

and appear in the phase of the monochromatic or finite pulse expression. It is sometimes called "phase anomaly near focus" since it causes the phase of a light wave to increase of π when passing through a focus. Because of the arctangent curve trend the entire variation of the phase occurs near the focus. Gouy himself wrote:

> If one considers a converging wave that has passed through a focus and has then become divergent, a simple calculation shows that the vibration of that wave has advanced half a period compared to what it should be according to the distance traveled and the speed of light.

The origin of the Gouy phase is a still debated question. It has been given the more different explanation, from classical ondulatory physics to quantum mechanics.

Temporal parameters We have already defined the duration of the pulse τ as:

$$\tau = \frac{2w_z}{c}.$$

Now we define the HWHM time $\tau_{\,\mathrm{HWHM}}$ as:

$$\tau_{\,\mathrm{HWHM}} = \frac{2L_{\,\mathrm{HWHM}}}{c}. \tag{3.21}$$

Using 3.9a and 3.9b For the Gaussian and the $\cos^2$ functions we get respectively:

$$\tau_{\,\mathrm{HWHM}} = 0,589\,\tau \tag{3.22a}$$

$$\tau_{\,\mathrm{HWHM}} = 0,364\,\tau. \tag{3.22b}$$

3.2 Graphical visualization

In this section we will give some graphical representation of the pulses, highlighting the condition in which they are valid approximations of the real solution of the wave equation. We will give some examples of the monochromatic pulses and of finite pulses, in the approximations we saw above. All plots are realized using the scaled coordinates 2.30, which appear to be more natural and simple than the usual ones.

We begin with giving the bidimensional plot of the monochromatic, Gaussian and $\cos^2$ pulse 2.37 in function of $z' = z/z_R$ for some values of the radius r.

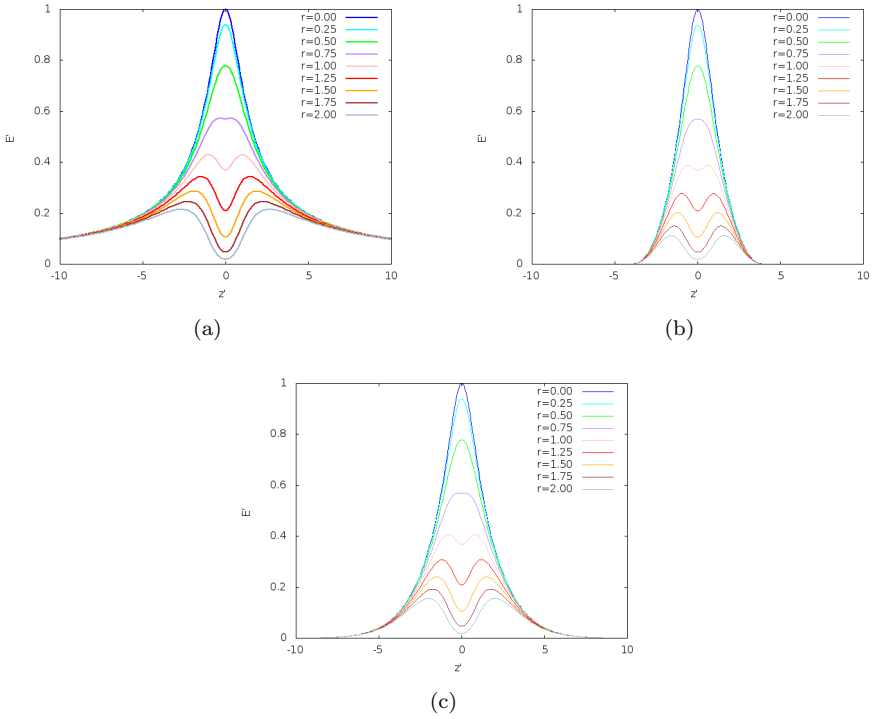

Figure 3.2: 3.2(a): Envelope of the monochromatic pulse in paraxial approximation. 3.2(b): Envelope of the finite pulse with a the $\cos^2$ shape function (factorization). 3.2(c): Envelope of the finite pulse with a Gaussian shape function (factorization). In all plots $w_0 = 4\,\mu$m and $\lambda_0 = 2\,\mu$m. In 3.2(b) and 3.2(c) we have chose $w_z = 4z_R$. (Note that the radii are the scaled radii $r' = r/w_0$).

For the three plots we have chose the transversal waist $w_0 = 4\,\mu$m and the central wave length $\lambda_0 = 2\,\mu$m. As a consequence the parameter $\epsilon \simeq 0,15 \sim 10^{-1}$, so that the error in applying the paraxial approximation is a $O(\epsilon^2) \sim 10^{-2}$. The Rayleigh length is $z_R \simeq 25\,\mu$m. Thus for 3.2(b) and 3.2(c) we have chose $w_z = 4z_R \simeq 100\,\mu$m and $z_R/w_z \simeq 0,25$. The Full Width Half Maximum time for the $\cos^2$ pulse is given by $\tau_{\,\mathrm{FWHM}} = 2\tau_{\,\mathrm{HWHM}} = 1,46\,w_z/c \simeq 500\,$fs.In that way the factorization 2.89 is a good approximation of 2.88. We will discuss the goodness of the factorized expression 2.89 compared to the integral 2.88 below.

We note that the monochromatic pulse goes to zero very slowly for $z' \to \infty$. The finite $\cos^2$ pulse, being shaped by a compactly supported function, is exacly zero for $|z'| \geq 4\,\mu$m. The finite pulse shaped by a Gaussian function goes to zero more rapidly than the monochromatic pulse but slowlier than the $\cos^2$ function.

In order to give an idea to what we are dealing with we give the plot of the $\cos^2$-shaped pulse with the parameters $w_0 = 4\,\mu$m, $\lambda_0 = 2\,\mu$m and $w_z = 2z_R \simeq 50\,\mu$m ($\tau_{\,\mathrm{FWHM}} \simeq 200\,$fs) and the color plot of the same pulse supplied with the same parameters.

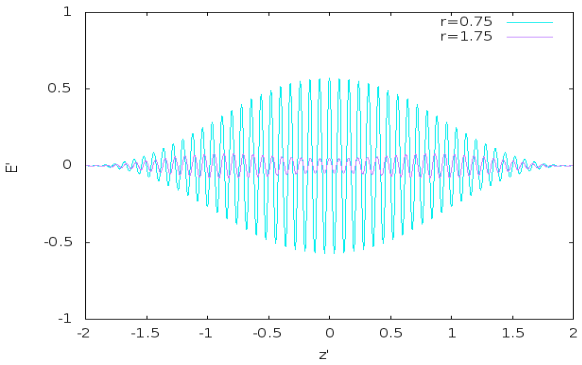

Figure 3.3: Finite pulse shaped by the $\cos^2$ function. We used $w_0 = 4\,\mu$m, $\lambda_0 = 2\,\mu$m, $w_z \simeq 50\,\mu$m, $\tau_{\,\mathrm{FWHM}} \simeq 200\,$fs. The field is given for two values of the radius: $r' = 0,75\,\mu$m, $r' = 1,75\,\mu$m. The number of the oscillations inside the pulse is given approximately by $2w_z/\lambda_0 = 4\pi w_0^2/\lambda_0^2 \simeq 47$.

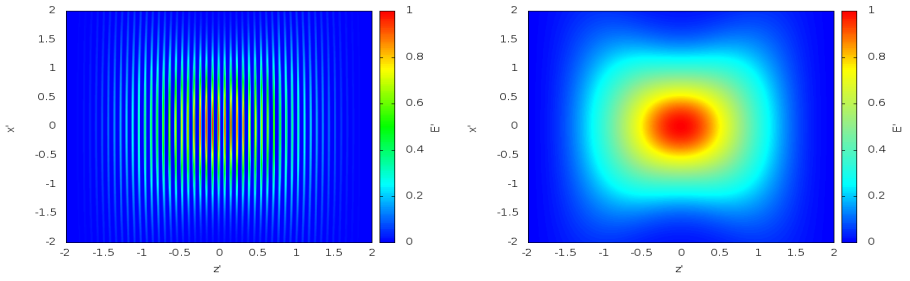

(a) (b)

Figure 3.4: 3.4(a): plot of the field E in the scaled coordinates x' and z'. 3.4(b): plot of the envelope of the field E in the same scaled coordinates. We used $w_0 = 4\,\mu$m, $\lambda_0 = 2\,\mu$m, $w_z \simeq 50\,\mu$m, $\tau_{\,\mathrm{FWHM}} \simeq 400\,$fs.

Figures 3.2(b) and 3.2(c) have been obtained from the factorized finite pulse 2.89. We have highlight that this approximation is valid for $w_z \gg w_0$. We give now some plot which describe the trends of a $\cos^2$ pulse with w_z changing, for four values of the radius r'. In our plots we have set $w_0 = 4\,\mu$m and $\lambda_0 = 2\,\mu$m again. In these conditions, because $z_R = 4\pi \simeq 25$, the request $w_z \gg w_0$ translates in the conditions that $w_z \geq z_R$, but w_z can be also that $w_z < z_R$. If it occurs that $w_z \ll z_R$ the approximation based on the factorization does not hold anymore.

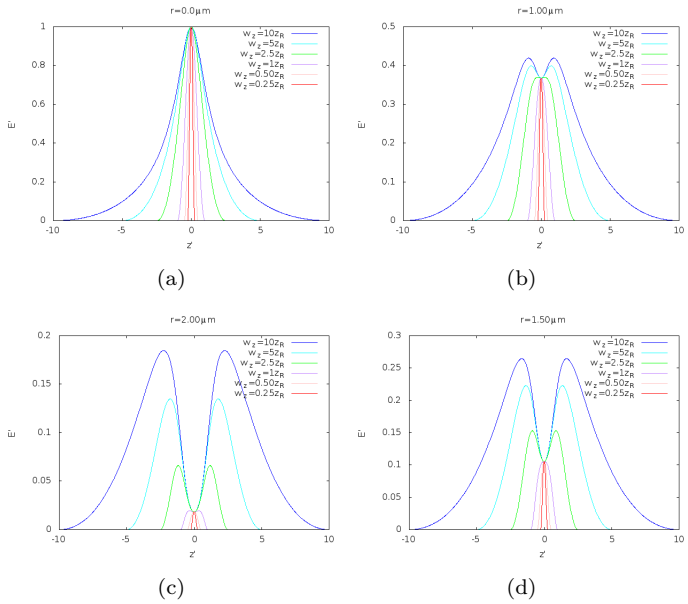

(a) (b)

(c) (d)

Figure 3.5: Envelope of the $\cos^2$ finite pulse for various values of w_z. The figures refers to different values of the radius r'. 3.5(a): $r' = 0\,\mu$m. 3.5(b): $r' = 1\,\mu$m. 3.5(c): $r' = 1.50\,\mu$m. 3.5(d): $r' = 2.00\,\mu$m. The colored lines refer to $w_z = 10z_R$, $5z_R$, $2.5z_R$, $1z_R$, $0.5z_R$, $0.25z_R$ which corresponds to $\tau_{\,\mathrm{FWHM}} = 1.2$ ps, 600 fs, 300 fs, 120 fs, 60 fs, 30 fs.

From 3.2(a)-3.2(c) we see that for a certain scaled radius $\bar{r}'$ there is a transition from an envelope with one maximum to an envelope with two maxima and one minimum. For the monochromatic pulse we can calculate the radius at which this transition happens and the coordinate $\bar{z}'$ at which the two maxima occurr. We make the substitution $u(z) = 1/w'(z') = (1 + z'^2)^{-1/2}$ so that the monochcromatic envelope can be written:

$$E'(r', u) = u\, \exp(-r'^2 u^2). \tag{3.23}$$

We have that the first and second derivative are given by:

$$\frac{\mathrm{d}u}{\mathrm{d}z'} = -\frac{2z'}{1 + z'^2}, \qquad \frac{\mathrm{d}^2 u}{\mathrm{d}z'^2} = \frac{2z'^2 - 2}{(1 + z'^2)^2}\,. \tag{3.24}$$

The first derivative of the field $E'(r', u)$ is:

$$\frac{\partial E'}{\partial z'}\big(r', u(z)\big) = (2u^2 r'^2 - 1)\exp(-u^2 r'^2)\,\frac{2z'}{1 + z'^2}. \tag{3.25}$$

The derivative given by expression 3.25 vanish either if $z' = 0$ or if $z' \neq 0$ and $(2u^2 r'^2 - 1) = 0$. The former case indicates that for all radii r' there is always a minimum or a maximum in $z' = 0$. The latter equations has real solutions only for

$$r' > \frac{1}{\sqrt{2}}, \qquad \text{i.e.} \qquad r > \frac{w_0}{\sqrt{2}}$$

and the solutions $\bar{z}'$ are given by

$$\bar{z}' = \pm\sqrt{2r'^2 - 1}. \tag{3.26}$$

If we calculate the second derivative in $z' = 0$ we see that it changes sign for $\bar{r}' = 1/\sqrt{2}$:

$$\left.\frac{\partial^2 E'}{\partial z'^2}\right|_{z'=0} = 2\exp(-r'^2)(2r'^2 - 1). \tag{3.27}$$

Paraxial approximation In Section 2.2 we shown how the introduction of the paraxial approximation to get an analytic expression for the monochromatic pulse brings about an error which goes to zero like $c\,\epsilon^2 = c\,\lambda_0^2/\pi^2 w_0^2$, where c is a constant to determine. The integral 2.59 can be computed using Gauss points method or the trapezoidal rule. Since the term $\sqrt{1 - K^2/k_0^2}$ which appears in the complex exponential can be either real or complex we have first to determine how to calculate it. There are two ways of considering the complex exponential, which we will call $g(z, K, k_0)$ for $t = 0$. We can set

$$g_1(z, K, k_0) = \exp\left[iz_r z'\sqrt{k_0^2 - K^2}\right]\theta(k_0 - K), \tag{3.28}$$

where θ is the Heaviside function, or

$$g_2(z, K, k_0) = \begin{cases} \exp\left[iz_r z'\sqrt{k_0^2 - K^2}\right], & k_0 > K \\ \\ \exp\left[-z_r|z'|\sqrt{k_0^2 - K^2}\right], & k_0 < K. \end{cases} \tag{3.29}$$

Using both these prescriptions we have calculated the relative and absolute error between the exact monochromatic solution 2.59 and the approximated solution 2.37, where we applied the paraxial approximation, by varying the transversal waist w_0, for fixed wave length λ_0. The error curves numerically obtained have been compared to the trend of the theorical curve $\epsilon^2(w_0) = \lambda_0^2/\pi^2 w_0^2$.All numerical calculations are performed using the expressions in the scaled variables 2.30. The exact integral 2.59 has been evaluated with the trapezoidal rule between 0 and 4. In fact, if we call I_4 the integral evaluated between these two extremes and I_∞ a simple calculation shows that:

$$I_\infty = I_4 + \exp(-4w_0^2). \tag{3.30}$$

Except a region of $w_0 \leq 1$ for which the error of numerical evaluation is comparable with unity, for $w_0 = 1$ the error is $\sim 10^{-2}$, for $w_0 = 2$ the error is $\sim 10^{-7}$ and for $w_0 = 4$ the error is $\sim 10^{-28}$.

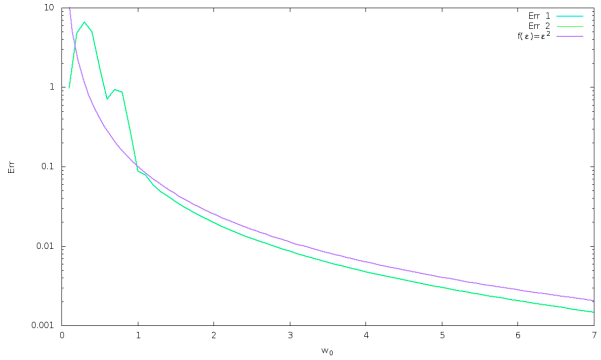

(a)

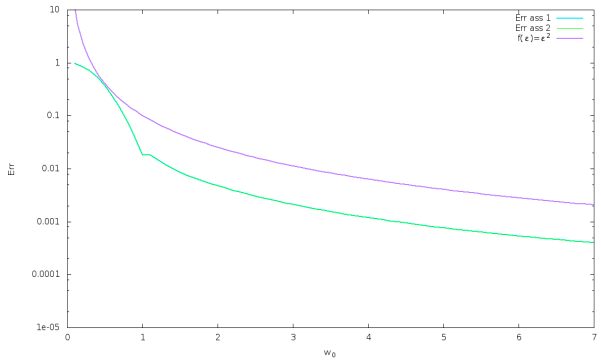

(b)

Figure 3.6: 3.6(a): Relative error between the exact monochromatic pulse and the paraxial-approximated monochromatic pulse. 3.6(b): Absolute error between the exact monochromatic pulse and the paraxial-approximated monochromatic pulse. A wave length $\lambda_0 = 1\,\mu$m has been used.

From 3.6(a) and 3.6(b) we see that the paraxial approximation falls inevitably for $w_0 \leq 1$. We note the perfect accordance between the theorical trend of the error and the numerical calculation. The relative error is very near to the theorical curve. This means that if we set

$$E_{\text{exact}} = E_{\text{parax}} + c\,\epsilon^2 \tag{3.31}$$

then the constant c is in order of magnitude comparable to E_{parax}, so that

$$E_{\text{exact}} \approx E_{\text{parax}}\,(1 + \epsilon^2). \tag{3.32}$$

In the following figures we show the color plots of the envelope of the monochromatic pulse calculated both in paraxial approximation and exactly with the functions g_1 and g_2. The wave length has been set to $\lambda_0 = 1\,\mu$m and the transversal waist has been given four values $w_0 = 4\,\mu$m, $1\,\mu$m, $0,5\,\mu$m, $0,25\,\mu$m.

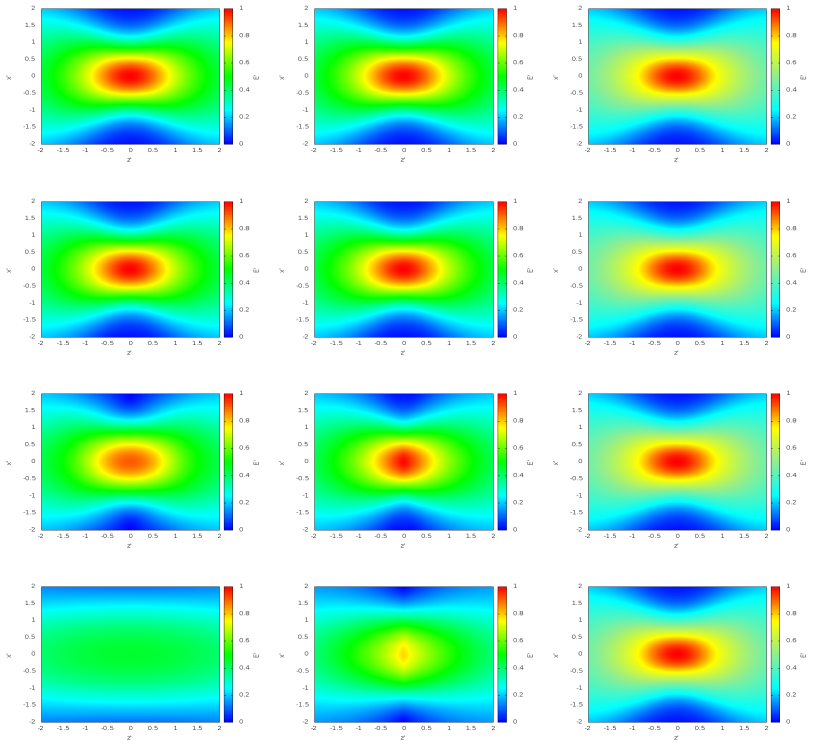

Figure 3.7: Comparison between the exact solution calculated with the prescription g_1 and g_2 (the two figures on the left for each series) and the paraxial-approximated solution (the figure on the right for each series). The parameters are $\lambda_0 = 1\,\mu$m (for all the series) and $w_0 = 4\,\mu$m, $1\,\mu$m, $0.5\,\mu$m, $0.25\,\mu$m (in order from top to bottom)

We can note how the approximated solution 2.37 distances from the real solution 2.59 as the ratio $\lambda_0/w_0 \sim \epsilon$ increases.

Factorization In Section 2.3 we have seen how we could approximate the integral

$$E_{\text{fin}}(x, y, z, t) = \frac{1}{2\pi} \int_{-\infty}^{+\infty} \mathrm{d}k_z \, E_0(x, y, z, t; k_z) \exp[ik_z(z - ct)] \, \hat{f}(k_z - k_0) \quad (3.33)$$

by the factorized expression

$$E_{\text{fin}}(x, y, z, t; k_0) = E_0(x, y, z, t; k_0) \, f(z - ct) \, \exp[ik_0(z - ct)] \quad (3.34)$$

if the Fourier transform $\hat{f}(k_z - k_0)$ of the shaping function $f(z)$ is sufficiently peaked in k_0. Of course, this factorization entails an error. We have already seen that this error get smaller as the ratio w_0/w_z (or z_R/w_0) decrease. In the next figures the trend of this error is investigated.

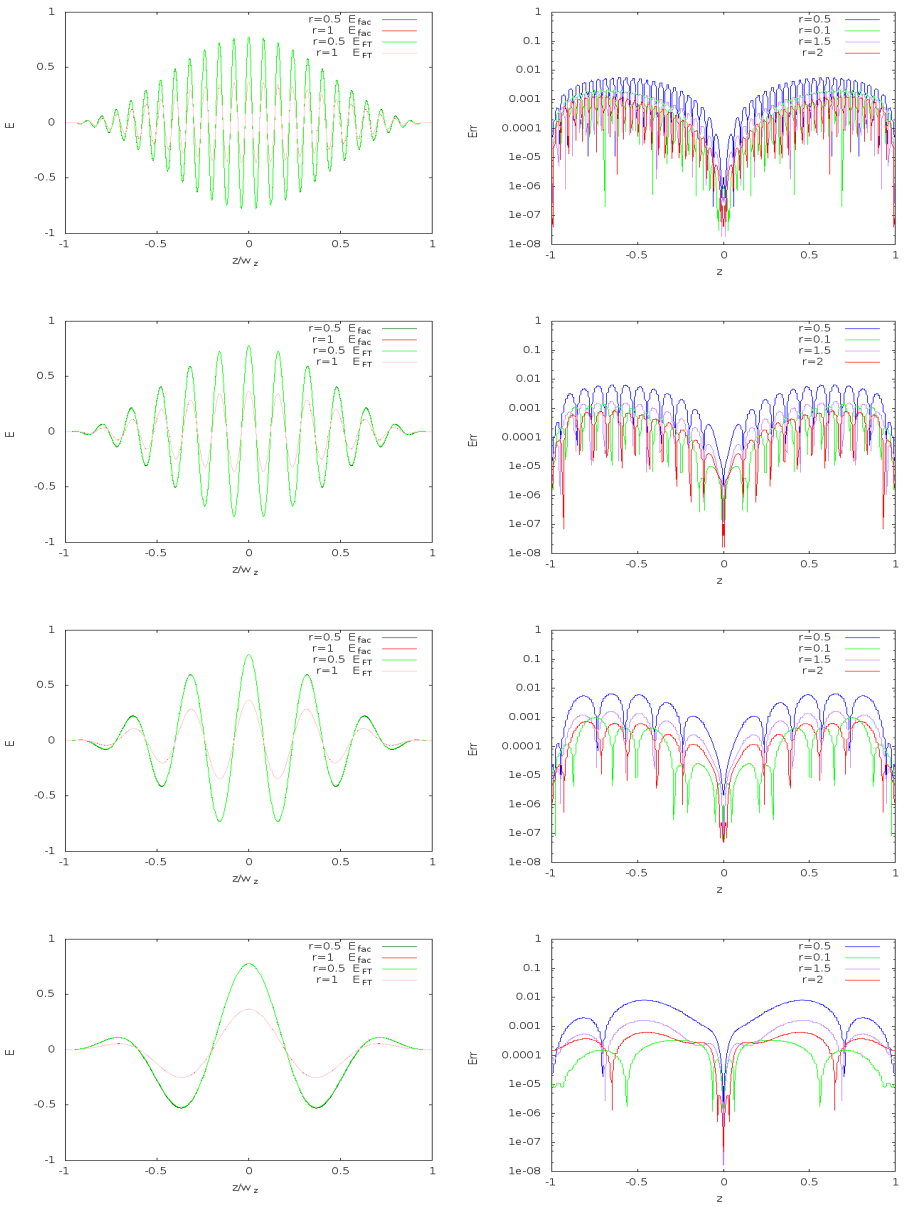

Figure 3.8: Left column: plot of the $\cos^2$ finite pulse by solving the integral 3.33 and by using the factorized expression 3.34. We used two values of the radius $r = 0.5\,\mu$m, $1\,\mu$m. Right column: Absolute error between the integral 3.33 and the factorized expression 3.34. We used four values of the radius $r = 0.5\,\mu$m, $1\,\mu$m, $1.5\,\mu$m, $2\,\mu$m. In all these figures $\lambda_0 = 1\,\mu$m and $w_0 = 2\,\mu$m. In order from top to bottom: $w_z = z_R$, $0.5z_R$, $0.25z_R, 0.1z_R$, which corresponds to $\tau_{\,\mathrm{FWHM}} = 61$ fs, 30 fs, 15 fs, 6 fs.

In the figures above we used the wave length $\lambda_0 = 1\,\mu$m and a transversal waist $w_0 = 2\,\mu$m. The parameters w_z , which defines the pulse duration has been set to $w_z = z_R$, $0.5z_R$, $0.25z_R, 0.1z_R$, which corresponds to a Full Width Half Maximum time of $\tau_{\,\mathrm{FWHM}} = 61$ fs, 30 fs, 15 fs, 6 fs. From the plots above is easy to see that, as we expected, the maximum of the absolute error calculated

in the z range tends to increase as the ratio w_z/z_R decrease.

Chapter 4

Motion of a charge in a one-dimensional field

In this final chapter we will explore some properties which concern the motion of a charged particle in a one-dimenional field in a relativistic regime, i.e., an electromagnetic field that depends only on the coordinate along with it propagates, say z. We will analyze the motion either in vacuum or in a plasma.

We will give a simple derivation of the ponderomotive force, already mentioned in the Introduction, by the point of view of the potential vector $\mathbf{A}$.

In order to understand the problem a general theoretical framework which makes use of Lagrangian and Hamiltonian mechanics will be given; the motion of charges in one-dimensional fields will be graphically illustrated by integrating the equations of motions and plotting the solutions.

From the plots which represent the motion of a charged particle in vacuum we will show the validity of Lawson-Woodward theorem, which states that, under certain conditions, it is impossible to accelerate a relativistic charge by direct-field interaction.

Unlike the particle in vacuum, when a particle propagates in a plasma, the Lawson-Woodward theorem is no more valid and the particle can be found to have gained energy after the passage of the pulse.

4.1 Charge in vacuum

4.1.1 Ponderomotive force

As we have already highlight in the Introduction the ponderomotive force plays a crucial role in laser-plasma acceleration. It is cause by the inhomogeneities of the electromagnetic field as a function of space. We now give a simple derivation of the ponderomotive force in the non-relativistic regime by the point of view of the potential vector. We will consider a electromagnetic pulse which propagates in the z direction and a vector potential with the only component in the y direction in the form

$$\mathbf{A} = A_{0y}(z,t)\cos(kz - \omega t)\hat{\mathbf{y}}. \tag{4.1}$$

In the non-relativistic regime the hamiltonian of a charged particle in a electromagnetic field in vacuum with no sources ($\phi = 0$) is given by:

$$\mathcal{H}(\mathbf{P}, \mathbf{x}, t) = \frac{1}{2m}\Big(\mathbf{P} - \frac{e}{c}\mathbf{A}\Big)^2, \tag{4.2}$$

where $\mathbf{P} = \mathbf{p} + e\mathbf{A}/c$, with $\mathbf{p}$ representing the ordinary momentum $\mathbf{p} = m\mathbf{v}$. We assume that at $t = 0$ the particle is at rest, so that $p_x = 0, \quad p_y = 0, \quad p_z = 0$. Then from Hamilton's equations of motion we find that $\dot{P}_x = -\partial\mathcal{H}/\partial x = 0$ and $\dot{P}_y = -\partial\mathcal{H}/\partial y = 0$. Thus $P_x = a$ and $P_y = b$, where a and b are constants. The force in the direction of propagation is given by:

$$F_z = \dot{P}_z = \frac{e}{mc}\left[\mathbf{P} - \frac{e}{c}A_{0y}(z,t)\cos(kz - \omega t)\hat{\mathbf{y}}\right]\cdot$$

$$\cdot\left[\frac{\partial A_{0y}}{\partial z}(z,t)\cos(kz - \omega t)\hat{\mathbf{y}} - kA_{0y}(z,t)\sin(kz - \omega t)\hat{\mathbf{y}}\right], \tag{4.3}$$

where in this case $\mathbf{P} = a\hat{\mathbf{x}} + b\hat{\mathbf{y}} + P_z\hat{\mathbf{z}}$. If we now make the scalar product and then average F_z over one period $T = 2\pi/\omega$ the unique contribution to the average is given by the $\cos^2$. Thus we find an expression for the average longitudinal force $\langle F_z\rangle$ which can be written:

$$\langle F_z\rangle = -\frac{e^2}{mc^2}\left\langle A_{0y}\frac{\partial A_{0y}}{\partial z}\cos^2(kz - \omega t)\right\rangle. \tag{4.4}$$

If A_y varies sufficienlty slowly within one period we can take out the term $A_{0y}\partial A_{0y}/\partial z$ from the angular brakets:

$$\langle F_z\rangle = -\frac{e^2}{2mc^2}A_{0y}\frac{\partial A_{0y}}{\partial z} = -\frac{e^2}{4mc^2}\frac{\partial}{\partial z}|\mathbf{A}|^2. \tag{4.5}$$

This is the expression of the ponderomotive force for a one-dimensional field. Generalizing and taking into account that $\mathbf{E} = -c^{-1}\partial\mathbf{A}/\partial t$ we have the ponderomotive force is given by $F_{\text{pond}} = -e^2/4mc^2\nabla|\mathbf{A}|^2 = -e^2/m\omega^2\nabla|\mathbf{E}|^2$.

4.1.2 Motion of a charge in a wave

We now want to obtain the equations of motion of a charged particle in a modulated electromagnetic field. We consider a linearly polarized wave which propagates in the z direction. We assume that the potential vector is in the form:

$$\mathbf{A}(z,t) = A_0 f(z - ct)\hat{\mathbf{y}}, \tag{4.6}$$

so that the only components of the electromagnetic field are

$$E_y = A_0 f'(z - ct) \tag{4.7}$$
$$B_x = -A_0 f'(z - ct), \tag{4.8}$$

where the derivative on f is taken with respect to the variable $z - ct$. The components of the forces given by:

$$F_y = eA_0 f'(z - ct) - \dot{z}\frac{eA_0}{c} f'(z - ct) \tag{4.9}$$
$$F_z = \dot{y}\frac{eA_0}{c} f'(z - ct). \tag{4.10}$$

Of course, in the real experiments of laser acceleration we have to use the framework of relativity, since the motion of the particle occurrs in the relativistic regime. The relativistic equation of motion are:

$$\begin{cases} m\dot{y} = p_y/\gamma \\ \\ m\dot{z} = p_z/\gamma \end{cases}, \qquad \begin{cases} \dot{p}_y = eA_0 f'(z - ct) - \dot{z}eA_0 f'(z - ct)/c \\ \\ \dot{p}_z = \dot{y}eA_0 f'(z - ct)/c \end{cases}, \tag{4.11}$$

where γ is the ordinary Lorentz factor:

$$\gamma = \left[1 - \frac{\dot{y}^2 + \dot{z}^2}{c^2}\right]^{-1/2}. \tag{4.12}$$

If the speed of the particle is not too high the Lorentz factor can be approximated by:

$$\gamma = \left[1 + \frac{p_y^2 + p_z^2}{m^2 c^2}\right]^{1/2}. \tag{4.13}$$

It is useful to introduced scaled adimensional variables, i.e., the spacial coordinates scale with the wave length λ, the time scales with T and the momentum scales with mc. Moreover, the normalized potential vector is defined as the ratio between the electromagnetic energy eA and the energy of the charge at rest:

$$a = \frac{eA}{mc^2}. \tag{4.14}$$

In the scaled variables the equations of motions read:

$$\begin{cases} \dot{y}' = p'_y/\gamma \\ \\ \dot{z}' = p'_z/\gamma \end{cases}, \qquad \begin{cases} \dot{p}_y = af'(\lambda(z' - t')) - ap'_z f'(\lambda(z' - t'))/\gamma \\ \\ \dot{p}_z = ap'_y f'(\lambda(z' - t'))/\gamma \end{cases}, \tag{4.15}$$

where in this case $f' = \mathrm{d}f/\mathrm{d}z'$ and $\gamma = (1 + p'^2_y + p'^2_z)^{1/2}$.

4.1.3 Hamiltonian formulation

We recall thet the generalized potential is $\tilde{V} = -e\,\mathbf{v}\cdot\mathbf{A}/c$ and that the lagrangian is written as:

$$\begin{aligned}\mathcal{L} &= -mc^2\gamma^{-1} + mc^2 - \tilde{V} \\ &= -mc^2\left[1 - \frac{\dot{y}^2 + \dot{z}^2}{c^2}\right]^{1/2} + mc^2 + \frac{eA_0}{c}\dot{y}f(z - ct). \end{aligned} \tag{4.16}$$

In the scaled variable the lagrangin is (for less than a multiplicative factor):

$$\mathcal{L}' = -(1 - \dot{y}^2 - \dot{z}^2)^{1/2} + 1 + a\dot{y}'f(\lambda(z' - t')). \tag{4.17}$$

From now on we abandon the prime notation to indicate the scaled variable. The hamiltonian can be computed after having calculated the conjugate momenta $P_y = \partial\mathcal{L}/\partial\dot{y} = p_y + af$ and $P_z = \partial\mathcal{L}/\partial\dot{z} = p_z$. Thus the hamiltonian is given by:

$$\begin{aligned}\mathcal{H} &= \gamma - 1 \\ &= (1 + p_y^2 + p_z^2)^{1/2} - 1 \\ &= \left[1 + (P_y - af)^2 + P_z^2\right]^{1/2} - 1. \end{aligned} \tag{4.18}$$

In order to get rid of the time dependence we can make a canonical transformation by using the generating function which depends on the old (scaled) coordinates and on new momenta $\hat{P}_y$ and $\hat{P}_z$:

$$F_1 = (z - t)\hat{P}_z + y\hat{P}_y, \tag{4.19}$$

which gives $\hat{z} = z - t$, $\hat{y} = y$, $\hat{P}_z = P_z$ and $\hat{P}_y = P_y$. The new hamiltonian $\hat{\mathcal{H}} = \mathcal{H} + \partial F_1/\partial t$ now reads:

$$\hat{\mathcal{H}} = \mathcal{H} - \hat{P}_z. \tag{4.20}$$

In this case the integrals of motion are $P_y = p_y + af$ and $\hat{\mathcal{H}}$, so that the equation of motion are:

$$\begin{cases} \dot{y} = (P_y - af)/\gamma \\ \\ \dot{z} = P_z/\gamma \end{cases}, \qquad \begin{cases} \dot{P}_y = 0 \\ \\ \dot{P}_z = a(P_y - af)f'(\lambda(z' - t'))/\gamma \end{cases}, \tag{4.21}$$

which are the same as 4.15.

4.1.4 Wave packet

We can choose, in the non-scaled variable

$$f(z) = \begin{cases} \cos(kz)S(z/l), & |z| \leq l \\ 0, & |z| > l. \end{cases} \tag{4.22}$$

In the scaled variables $z' = z/\lambda$ and $l' = l/\lambda$, since $k = 2\pi/\lambda$, the same equation reads:

$$f(z') = \begin{cases} \cos(2\pi z')S(z'/l'), & |z'| \leq l' \\ 0, & |z'| > l'. \end{cases} \tag{4.23}$$

S is a symmetrical function and the condition $S(\pm 1) = 0$ must hold. We choose here $S(z'/l') = \cos(\pi z'/2l')$. We note that in the scaled variables the function f has a wave length equal to 1 while the modulation has a wave length equal to $2l'$. If the condition $l' \gg 1$ holds we can approximate the motion of the particle in the wave packet by using the equations of motion obtained from the average hamiltonian. In case of relativistic motion the further condition that the longitudinal momuntum is much greater than the transversal momentum must hold:

$$|p_y| = |P_y - af| \ll |P - z| = |p_z|. \tag{4.24}$$

The necessity of this condition will become clearer in the next mathematical passages. We next calculate the average of the relativistic hamiltonian 4.18.

$$\begin{aligned} \langle \mathcal{H} \rangle &= \left\langle \sqrt{1 + (P_y - af)^2 + P_z^2} \right\rangle - 1 \\ &= \left\langle \sqrt{1 + P_z^2} \sqrt{1 + \frac{P_y - af}{1 + P_z^2}} \right\rangle - 1 \\ &\simeq \sqrt{1 + P_z^2} \left\langle 1 + \frac{1}{2} \frac{(P_y - af)^2}{1 + P_z^2} \right\rangle - 1 \\ &\simeq \sqrt{1 + P_z^2} \left[1 + \frac{1}{2} \frac{P_y^2 + a^2 \langle f^2 \rangle}{1 + P_z^2} \right] - 1 \\ &\simeq \sqrt{1 + P_z^2 + P_y^2 + a^2 \langle f^2 \rangle} - 1. \end{aligned} \tag{4.25}$$

If we choose $S(z'/l') = \cos(\pi z'/2l')$ the equations of motions become:

$$\begin{cases} \dot{y} = P_y/\gamma \\ \\ \dot{z} = P_z/\gamma \end{cases} , \qquad \begin{cases} \dot{P}_y = 0 \\ \\ \dot{P}_z = \frac{a^2}{2\gamma}\frac{\pi}{4l}\sin\left[\frac{\pi}{l}(z-t)\right] \end{cases} . \tag{4.26}$$

In the next figures we have plotted, both in configuration space and in phase space, the motion of a charged particle which interacts with a one-dimensional field of the kind 4.23 in a relativistic regime with $a = 4$.

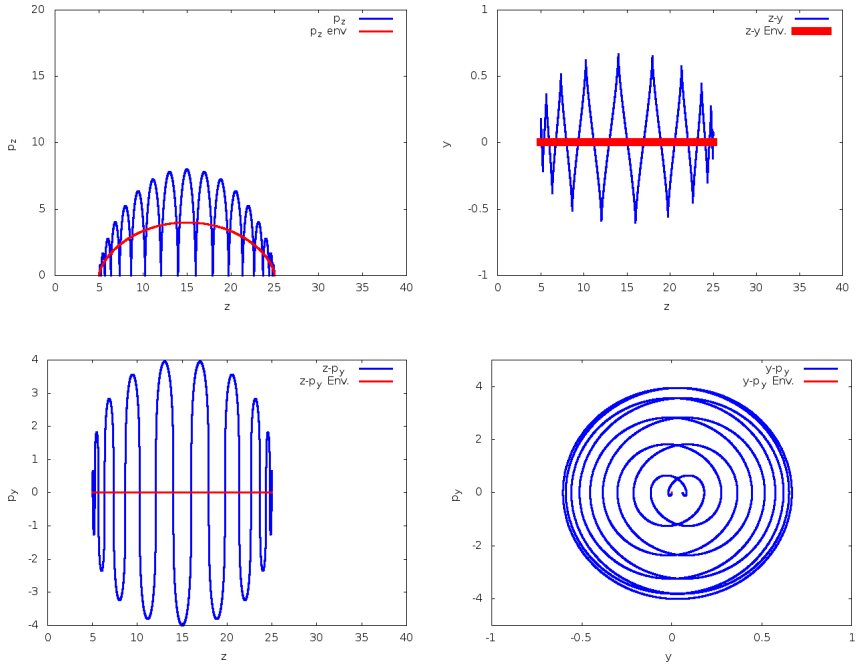

Figure 4.1: Top left: phase space of longitudinal momentum and coordinate. Top right: configuration space of the coordinates y ans z. Bottom left: phase space of the transversal momentum p_y and the longitudinal coordinate z. Bottom right: phase space of the transvesal momentum and coordinate. In all figures it is shown either the exact motion and the envelope approximation. The motionis in a relativistic regime $a = 4$.

Figures 4.1 show graphucally the validity of Lawson-Woodward theorem. In fact, if the particle interacts with a one-dimensional field and the potential vector has only one component in a direction orthogonal to the propagation direction which depends only on z and t in turn (for instance $\mathbf{A} = A_y(z,t)\hat{\mathbf{y}}$), after the passage of the pulse the particle has not gained momentum.

4.2 Propagation in a plasma

If the propagation of the wave packet occurrs in a plasma the wave equation for the y component of the potential vector reads:

$$\frac{\partial^2 A_y}{\partial z^2} + \frac{1}{c^2}\frac{\partial^2}{\partial t^2} = J_y(A_y) = \frac{\chi(y)}{\lambda_0} A_y. \tag{4.27}$$

If we make the scaling:

$$z' = \frac{z}{\lambda_0}, \qquad t' = \frac{t}{T}, \qquad a = \frac{eA_y}{mc^2}, \qquad p'_z = \frac{p_z}{mc} \tag{4.28}$$

and neglect second order terms we obtain the equation for the potential:

$$\frac{\partial^2 A_y}{\partial z'^2} - \frac{\partial^2 A_y}{\partial t'^2} = \chi_0 a. \tag{4.29}$$

As in the previous section, in the scaled variables we choose:

$$a(z', t') = a_0 \cos[2\pi(z' - t')] B\left(\frac{z' - t'}{w'_z}\right), \tag{4.30}$$

where we have set $w'_z = w_z/\lambda_0$ and $B(x) = 0$ for $|x| > 1$ and $B(x) = \cos(\pi x/2)$ for $|x| < 1$. From now on we remove the prime symbol from the variables and we will mean the scaled variables.

If $\hat{B}(k_z)$ is the Fourier transform of $B(z/w_z)$ then the Fourier transform of $a(z, 0)$ is given by $\hat{B}(k_z - k_0)$, where in the scaled variables $k_0 = 2\pi$. The expression which satisfies 4.29 is given by:

$$a(z, t) = \frac{a_0}{2\pi} \int_{-\infty}^{+\infty} \mathrm{d}k_z \exp\left[k_z z - \sqrt{k_z^2 - \chi_0^2}\, t\right] \hat{B}(k_z - k_0). \tag{4.31}$$

The integral gives its main contribution in an interval $|k_z - k_0| < 1/w_z$. If we set $k_z = k_0 + u$ we can re-write the solution:

$$a(z, t) = \mathfrak{Re}\, a_0 e^{ik_0(z-t)} \frac{1}{2\pi} \int_{-\infty}^{+\infty} \mathrm{d}u \exp\left[iuz - it\Big(\sqrt{(k_0 + u)^2 - \chi_0^2} - k_0\Big)\right] \hat{B}(u). \tag{4.32}$$

If we assume $\chi_0 \ll k_0$ and $w_z \gg 1$ we can make the expansion:

$$\begin{aligned}
\sqrt{(k_0 + u)^2 - \chi_0^2} - k_0 &= k_0 \left[\left(1 + \frac{2u}{k_0} + \frac{u^2}{k_0^2} - \frac{\chi_0^2}{k_0}\right)^{1/2} - 1\right] \\
&= k_0 \left[\frac{u}{k_0} + \frac{u^2}{2k_0^2} - \frac{\chi_0^2}{2k_0^2} - \frac{u^2}{2k_0^2} + O(u^3)\right] \\
&= u - \frac{\chi_0^2}{2k_0} + O(u^3).
\end{aligned} \tag{4.33}$$

If we neglect third order terms and define $c_0 = 1 - \chi_0^2/2k_0^2 \simeq \sqrt{1 - \chi_0^2/k_0^2}$ we get:

$$a(z,t) = \mathfrak{Re}\, a_0 e^{ik_0(z-c_0t)} \frac{1}{2\pi} \int_{-\infty}^{+\infty} \mathrm{d}u \exp(iuz)\hat{B}(u)$$

$$= a_0 \cos[2\pi(z - c_0t)]B(z - t). \tag{4.34}$$

Since $a(z,t) = a_0 \cos[2\pi(z - c_0t)] \cos(\pi z/2w_z)$ and since the equations of motions are given by:

$$\dot{p}_y = -\frac{\partial a}{\partial t} - \dot{z}\frac{\partial a}{\partial z}$$

$$\dot{p}_z = \dot{y}\frac{\partial a}{\partial z} \tag{4.35}$$

we get:

$$\dot{p}_y = -2\pi a_0 c_0 \sin[2\pi(z - c_0t)] \cos\left(\frac{\pi}{2}\frac{z-t}{w_z}\right) - \frac{\pi a_0}{2w_z} \cos[2\pi(z - c_0t)] \sin\left(\frac{\pi}{2}\frac{z-t}{w_z}\right)$$

$$+ 2\pi a_0 \dot{z} \sin[2\pi(z - c_0t)] \cos\left(\frac{\pi}{2}\frac{z-t}{w_z}\right) + \dot{z}\frac{\pi a_0}{2w_z} \cos[2\pi(z - c_0t)] \sin\left(\frac{\pi}{2}\frac{z-t}{w_z}\right) \tag{4.36}$$

$$\dot{p}_z = -2\pi a_0 \dot{y} \sin[2\pi(z - c_0t)] \cos\left(\frac{\pi}{2}\frac{z-t}{w_z}\right) - \dot{y}\frac{\pi a_0}{2w_z} \cos[2\pi(z - c_0t)] \sin\left(\frac{\pi}{2}\frac{z-t}{w_z}\right) \tag{4.37}$$

If we now plot the energy gain (p_z) after the pulse have passed ($t - z > w_z$ as a function of c_0 we find that it is possible for the particle to have a finite momentum in the longitudinal direction. This did not occurr for a single particle in a one-dimensional electromagnetic field.

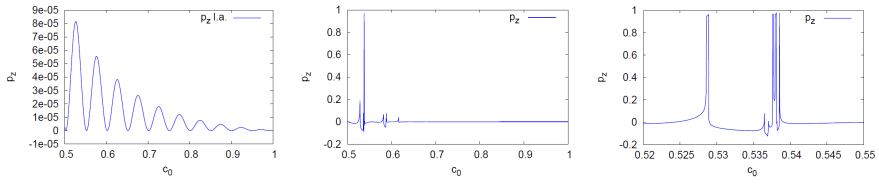

Figure 4.2: Longitudinal momentum of the particle after the passage of the wave packet. Left: $a_0 = 0.2$. Center: $a_0 = 1$. Right: detail of the previous figure.

In the next two figures we have compared the motion of a charged particle which interacts with a one-dimensional wave packet in vacuum and the motion of a charged particle in a plasma.

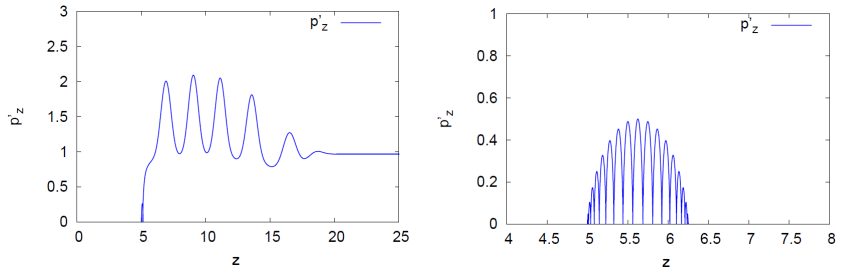

Figure 4.3: Left: motion of a charged particle in a plasma. The final momentum is $p_z \simeq$ mc which corresponds to an energy of $E_p \simeq 1$ Mev or $E_e \simeq 0.5$ Mev for an electron. Right: motion of a charged particle in vacuum. The final momentum is $p_z = 0$.

Conclusions

In this work we have analyzed the propagation of a Gaussian pulse either in the monochromatic case (with frequency $\omega_0 = k_0 c$) and in the case of a finite pulse, which is a wave modulated by a function $f(z)$, where z is the longitudinal coordinate of propagation. The monochromatic wave is a stationary solution of the electromagnetic wave equation in vacuum. Physically it represents a long beam focalized in the origin $z = 0$. Unlike the monochromatic pulse, the finite pulse is not a stationary solution and it represents a wave whose envelope propagates in space along the z direction. Of course, in real experiments we always deal with finite pulses. The main results of this thesis concern the limits for the accuracy of the paraxial approximation for monochromatic pulses and the ones for the validity of the factorization approximation for finite pulses. At the end we have shown how the motion of a charged particle is different depending on where it propagates, in vacuum or in a plasma.

The analytical expressions 2.37 or 2.47 for the monochromatic pulse are correct up to orders of $\epsilon^2 = \lambda_0/\pi w_0$. If we choose $\lambda_0 = 0.8\,\mu$m, which are the typical wave length of a Ti:Sa laser, we get that the relative error is of the order of 1%, if the transversal waist is just $w_0 = 3\,\mu$m. In fact, comparing the curve of the relative error between the exact solution and the approximated one as a function of w_0 and the curve of $\epsilon^2 = \epsilon^2(w_0)$ (plot 3.6) we have noticed that the curve of the relative error is very near to that of ϵ^2. We can identify the relative error $|E_{\text{exact}} - E_{\text{mono}}|/|E_{\text{mono}}|$ with ϵ^2 with good accuracy. We have numerically verified the accuracy of paraxial approximation by integrating the exact solution and plotting the approximated one. By the plots it can be seen that, while w_0 gets smaller the accordance between the exact solution and the approximated one fails.

When the pulse is longitudinally modulated by a function $f(z)$ (in our work we have taken into account the case $f(z) = \cos^2(\pi z/2w_z)$, which is a function often chosen in literature) we are dealing with a wave packet which propagates in the z direction. In this case we have equation 2.88 for the finite pulse, where E_0 is the envelope of the field in paraxial approximation and $\hat{f}(k_z)$ the Fourier transform of $f(z)$. In this case we have found that if $\hat{f}(k_z - k_0)$ is sufficiently peaked in k_0 we can approximate 2.88 with the factorized expression 2.89. In fact, searching for the envelope wave equation satisfied by the factorized filed, we found that the factorization approximation is accurate if we have pulses of long duration ($w_z \geq z_R$). By 2.91 we see that the error is of the order of w_0^2/w_z^2. and for short pulses and for low focusing the error introduced by the factorization can be important. For a real Ti:Sa laser with $\tau_{\text{FWHM}} = 30 - 40\,$fs and a high focusing $w_0 = 2 - 3\,\mu$m we have that $w_z = 6 - 8\,\mu$m (for the $\cos^2$ function)

and $w_0^2/w_z^2 \sim 0,1$ and we can consider the factorization a good approximation. For instance, in electron acceleration, there is low focusing $w_0 \simeq 10$ and the factorization is no longer valid.

In the paraxial approximation the Gaussian monochromatic pulse is not the unique solution of the envelope equatio 2.52. In fact, we have considered also the Hermite-Gauss and Laguerre-Gauss modes, beyond the fundamental mode. These modes correspond to physically reproducible situations. The validity of the paraxial approximation for monochromatic pulse and of the factorization for the finite pulse discussed so far is the same also for this higher harmonics.

In the last chapter we have highlight the difference between the motion of a charged particle which interacts with a one-dimensional field in vacuum and a particle whose motion due to the same field occurrs in a plasma. The main difference is that the particle which moves in vacuum cannot gain energly, since after the passage of the wave packet its momentum along the direction of propagation of the pulse is zero (if at the initial time its momentum was zero). When a particle moves into a plasma it is possible for tha particle to gain energy and so to be accelerated by the passage of the wave packet.

Summarizing, the paraxial approximation for monochromatic pulses provide a rather accurate analytical expression if the parameter $\epsilon = \lambda_0/\pi w_0 \ll 1$, while it fails beyond the diffraction limit $w_0 < \lambda_0$. As concerns the finite pulse the factorization approximation is valid for long and focalized pulses. Analyzing the motion of a particle which interacts with a one-dimensional field we found that it gains no energy if the motion occurrs in vacuum, while it is possible for it to gain momentum if the motion occurrs in a plasma.

Bibliography

[1] J. P. Barton and D. R. Alexander, *Fifth-order corrected electromagnetic field components for a fundamental gaussian beam*, Journal of Applied Physics **66** (1989), no. 7, 2800–2802.

[2] Claudio Chiuderi and Marco Velli, *Fisica del plasma: Fondamenti e applicazioni astrofisiche*, UNITEXT - Collana de Fisica e Astronomia, Springer, Milano, 2012.

[3] S. Corde, K. Ta Phuoc, G. Lambert, R. Fitour, V. Malka, A. Rousse, A. Beck, and E. Lefebvre, *Femtosecond X rays from laser-plasma accelerators*, Reviews of Modern Physics **85** (2013), 1–48.

[4] H. Daido, M. Nishiuchi, and A. S. Pirozhkov, *Review of laser-driven ion sources and their applications*, Reports on Progress in Physics **75** (2012), no. 5, 056401.

[5] Simin Feng and Herbert G. Winful, *Physical origin of the gouy phase shift*, Opt. Lett. **26** (2001), no. 8, 485–487.

[6] A. Gamucci, *Produzione e caratterizzazione di plasmi per esperimenti su nuove tecniche di accelerazione di elettroni*, Master's thesis, University of Pisa, 2004–2005.

[7] Hyo-Chang Kim and Yeon H. Lee, *Hermite-gaussian and laguerre-gaussian beams beyond the paraxial approximation*, Optics Communications **169** (1999), no. 1-6, 9 – 16.

[8] A. Macchi, M. Borghesi, and M. Passoni, *Ion acceleration by superintense laser-plasma interaction*, ArXiv e-prints (2013).

[9] F. Pampaloni and J. Enderlein, *Gaussian, Hermite-Gaussian, and Laguerre-Gaussian beams: A primer*, ArXiv Physics e-prints (2004).

[10] A. Popp, *Dynamics of electron acceleration in laser-driven wakefields: acceleration limits and asymmetric plasma waves*, Ph.D. thesis, University of München, 2011.

[11] Brice Quesnel and Patrick Mora, *Theory and simulation of the interaction of ultraintense laser pulses with electrons in vacuum*, Phys. Rev. E **58** (1998), 3719–3732.

[12] Bernhard Rau, T. Tajima, and H. Hojo, *Coherent Electron Acceleration by Subcycle Laser Pulses*, Phys.Rev.Lett. **78** (1997), 3310–3313.

[13] H. P. Schlenvoigt, O. Jäckel, S. M. Pfotenhauer, and M. C. Kaluza, *Laser-based particle acceleration*, Advances in Solid State Lasers Development and Applications (M. Grishin, ed.), Intech, 2010.

[14] C. B. Schroeder, C. Benedetti, E. Esarey, J. van Tilborg, and W. P. Leemans, *Group velocity and pulse lengthening of mismatched laser pulses in plasma channels*, Physics of Plasmas **18** (2011), no. 8, 083103+.

[15] A. Sgattoni, *Equazioni di maxwell-liouville ed accelerazione di cariche tramite un impulso elettromagnetico*, Master's thesis, University of Bologna, 2005–2006.

[16] A. Sgattoni, *Theoretical and numerical study of the laser-plasma ion acceleration*, Ph.D. thesis, University of Bologna, 2011.

[17] Stefano Sinigardi, Giorgio Turchetti, Pasquale Londrillo, Francesco Rossi, Dario Giove, Carlo De Martinis, and Marco Sumini, *Transport and energy selection of laser generated protons for postacceleration with a compact linac*, Phys. Rev. ST Accel. Beams **16** (2013), 031301.

[18] G. Turchetti, *Dinamica classica dei sistemi fisici*, Collana di fisica. Testi e manuali, Zanichelli, 1998.

[19] Emil Wolf and Taco Visser, *The origin of the gouy phase anomaly and its generalization to astigmatic wavefields*, Frontiers in Optics 2010/Laser Science XXVI, Optical Society of America, 2010, p. FThV3.